

Master Thesis in Marine Microbiology

University of Bremen



HOW DO PRO- AND EUKARYOTIC MICROBIAL COMMUNITIES IMPACT NITROGEN AND CARBON PROCESSES IN THE SOUTH INDIAN OCEAN AND THE FRENCH SOUTHERN AND ANTARCTIC LANDS?

A thesis submitted in partial fulfillment of requirements for the degree of

Master of Science (M.Sc.)

Submitted by

Cora Hörstmann

Bremen, 2018

Reviewers:

Prof. Dr. Anya Waite

PD Dr. Bernhard Fuchs

Supervisor in the lab:

Dr. Eric J. Raes



HOW DO PRO- AND EUKARYOTIC MICROBIAL COMMUNITIES IMPACT NITROGEN AND CARBON PROCESSES IN THE SOUTH INDIAN OCEAN AND THE FRENCH SOUTHERN AND ANTARCTIC LANDS?

Master Thesis in Marine Microbiology

University of Bremen

Cora Hörstmann

Bremen, 2018

Reviewers:

Prof. Dr. Anya Waite

PD Dr. Bernhard Fuchs

Supervisor in the lab:

Dr. Eric J. Raes

Abstract

Nitrogen availability in the open ocean regulates primary productivity and a cascade of associated carbon-nitrogen coupled transformations mediated by both eukaryotic and prokaryotic microorganisms. An understanding of potential alterations at the base of the food chain particularly reductions in planktonic biomass is essential, as a decline or community shift in primary productivity will impact ecosystem services, such as O₂ production, carbon sequestration and biogeochemical cycling. This study, as part of the OISO (Ocean Indien Service d'Observation) campaign, aimed to shed light into prokaryotic and photoautotrophic, eukaryotic community composition between four different water masses as well carbon and nitrogen assimilation rates in the Southern Indian Ocean and the French Southern and Antarctic lands. To understand ecosystem dynamics, we linked microbial community composition, using high resolution molecular 16S rDNA amplicon sequencing techniques and functional pigment analysis, to *in situ* rate measurements of carbon (C) and nitrogen (N). While temperature and salinity were the driving factors for carbon fixation, water masses defined prokaryotic community composition. We could link prokaryotic diversity to high carbon fixation rates emphasizing positive foodweb recoupling and recycling processes. Photoautotrophic community composition clearly separated between the warm Indian Ocean and the Southern Ocean. While the Indian Ocean was vastly dominated by the unicellular cyanobacterium *Prochlorococcus*, the relative abundance of the diatom diagnostic pigment fucoxanthin increased in the Southern Ocean. C fixation was relatively higher ($84.8 \pm 44.5 \mu\text{mol L}^{-1} \text{h}^{-1}$) in the nutrient-rich Southern Ocean, in comparison to the oligotrophic Indian Ocean ($14.2 \pm 7.9 \mu\text{mol L}^{-1} \text{h}^{-1}$). In general, high variations within-station replicates of C fixation were found, ranging from $43.4 - 134.9 \mu\text{mol L}^{-1} \text{h}^{-1}$. We measured N₂ fixation at all sampling stations, up to 56°S latitude, supporting the hypothesis that N₂ fixation is an ubiquitous process which is not restricted to warm oligotrophic water. N₂ fixation rates showed similar patterns as C fixation rates within station replicates, ranging from 0.9 to 7.9 nmol N L⁻¹ d⁻¹. Among other interpretations, this suggests sub-mesoscale dynamics and potential small-scale differences in biochemical conditions. Our observations point out the importance of high resolution (i.e., sub-mesoscale and smaller) *in situ* studies in combination with remote-sensing techniques, to be able to fully understand the scale of variation in ocean dynamics.

Collectively our results are another piece of the puzzle of the complex dynamics in the Southern Indian Ocean sector. Understanding biogeochemical and biological processes supports our ability to further understand C and N fluxes to be able to predict and model future climate change scenarios.

Table of Contents

Abstract	i
List of figures and tables	v
List of major abbreviations.....	viii
1. Introduction.....	1
1.1 The Southern Indian Ocean and Southern Ocean	1
1.2 The Nitrogen Cycle.....	2
1.3 Aims of this Study	4
2. Materials and Methods	6
2.1 Sampling strategy	6
2.2 Perturbation experiments	8
2.3 Biophysical data	9
2.4 Nutrient Analysis	9
2.5 Functional pigment analysis	10
2.6 Microbial diversity analysis based on 16S rDNA	11
2.6.1 Amplicon 16S PCR	11
2.6.2 Amplicon nifH PCR	12
2.6.3 Index PCR	12
2.6.4 Sequencing and data analysis	12
2.7 N ₂ fixation rates	13
2.8 Carbon and Nitrogen assimilation experiments.....	14
2.9 Statistical analysis	15
3. Results	16
3.1 Hydrographic conditions.....	16
3.2 Nutrient distributions	18
3.3 Carbon and Nitrogen fixation rates	20
3.4 Community composition	25
3.4.1 Autotrophic pigment analysis based on High Performance Liquid Chromatography	25
3.4.2 16S rDNA amplicon sequence analysis	29
4. Discussion	30
5. Conclusion	35

Acknowledgement.....	36
References.....	37
Appendix.....	56

List of figures and tables

FIGURES

- Figure 1:** Marine nitrogen cycle. New nitrogen input from (1) river runoff and (2) autotrophic and heterotrophic nitrogen fixation. (3) Ammonium can be oxidized to nitrite and nitrate by nitrifying microbes. Ammonium and nitrate can be taken up by phytoplankton (4) and transferred to higher trophic levels (5). Decomposing microbes can turn organic N (N_{org}) into Ammonium (6). Under suboxic conditions, nitrate can be reduced to Nitrite and N_2 by denitrifying microbes (7); Anammox (anoxic ammonium oxidation) microbes can oxidize ammonium using nitrite as electron acceptor to N_2 (8)..... 3
- Figure 2:** Schematic overview of experimental setup. Incubations were done in triplicates for each enrichment (NO_3^- , NH_4^+ , N_2 and $NaHCO_3$). TO as well subsamples from the incubations were taken for HPLC, DNA and DIN analysis in two different incubation bins 7
- Figure 3:** Schematic of incubation setup. Water inflow from ship underway system. Arduino continuously measured temperature in both bins. 7
- Figure 4:** Temperature continuously measured in incubation bins (blue line bin 1, red line bin 2) and sporadically for sea surface temperature (SST) (black dots). Arrows indicate where ship was crossing different fronts; yellow arrows highlight indian ocean (IO), blue arrows indicate Antarctic circumpolar current (ACC) and green arrow highlights polar front (PF) 8
- Figure 5: A,** Map of sampling stations within different water masses, water masses modified from Park et al 2008(b); **B,** Temperature- salinity plot differentiating these water masses. Mixed water is encircled with dashed lines. 16
- Figure 6:** Depth profiles of temperature, oxygen and salinity along two transects of the OISO stations. **A-C,** covering OISO stations 2, 3, 6 and 37; a clear difference in all parameters is shown between IO and ACC. **D-F,** show latitudinal transect of OISO stations E. Blue arrows highlight the Antarctic circumpolar current (ACC), green arrow the Polar Front (PF) and yellow arrows the Indian Ocean (IO). 17
- Figure 7:** Nutrient and DIC concentration against sea surface temperature (SST) over the past 19 years. Trendlines 4th polynomial fit. **A,** nitrate concentration in $\mu\text{mol L}^{-1}$. **B,** phosphate concentration in $\mu\text{mol L}^{-1}$ **C,** Silicate concentration in $\mu\text{mol L}^{-1}$. **D,** DIC concentration in $\mu\text{mol kg}^{-1}$ 19
- Figure 8:** Carbon and nitrogen fixation rates against sea surface temperature (SST) from two different incubation bins with three replicates each. **A,** carbon fixation, followed a trend with relative high rates in the mixing zone between IO and ACC; trendline: $R^2 = 0.5$. **B,** chlorophyll a- normalized, specific carbon fixation rate against SST; **C,** Ammonium assimilation. **D,** Nitrate fixation rates having

relatively higher rates in the warm water of the IO. Arrows indicate major fronts as described for figure 6. 22

Figure 9: Relationships between particulate organic matter (POM) composition and sea-surface temperature (SST). **A**, Natural abundance of $\delta^{15}\text{N}$ from the particulate organic nitrogen (PON). Red lines are smoothing curves with a second polynomial order. **B**, POC: PON ratios in POM. 23

Figure 10: Nitrogen fixation rates shown in $\text{nmol N L}^{-1} \text{d}^{-1}$. Grey bar indicates minimum quantifiable rate ($\text{MQR} = 0.8 \text{ nmol N L}^{-1} \text{d}^{-1}$). 23

Figure 11: pigment analysis, showing **(A)** the relationship of different pigment concentrations for each station at T0 and T24. Stations are ordered according to their SST (non-linear). Arrows indicate changes of water masses. **B**, pigment concentrations normalized by total pigment concentration. .. 25

Figure 12: Phytoplankton functional types (PFTs) and Phytoplankton size classes (PSCs) against SST. **A**, relative abundance of different PFTs calculated after Hirata et al. (2011), stations are sorted after increasing temperature. **B**, relative abundance of size classes against SST calculated after Uitz et al. (2006). Brown arrow highlights the mixed water between PF and Fawn Trough, green arrow PF, dark blue arrow ACC, light blue arrow mixed water of ACC and IO and yellow arrow IO 26

Figure 13: Microbial photoautotrophic community structure of different water masses. Constrained Analysis of Principal Coordinates (CAP) of pigment concentrations (HPLC). Pigment concentrations were used to calculate Bray- Curtis distances and constrained analysis was performed by water mass. Constrain reflects 84.4 % of overall variance in the data. There was a significant relationship between water masses and community dissimilarity (adonis test; $p < 0.001$). Different water masses were coloured according to the legend; water mass (WM); Indian Ocean (IO); mixed water of Indian Ocean and Antarctic Circumpolar Current (IO/ACC); Antarctic Circumpolar Current (ACC); Polar Front (PF) and mixed water of Polar Front and Fawn Trough (PF/Fawn Trough). Data with environmental samples represented as arrows. 27

Figure 14: **A**, OTU richness of 16S amplicon sequences changing over SST. **B**, Alpha diversity of OTUs calculated as inverse Simpson Index against SST. Arrows indicate major fronts as described in figure 6. 29

Figure 15: **A**, relative abundance of phyla for each station and within incubations. Arrows indicate major water masses according to the legend; Indian ocean (IO), mixed water of Indian Ocean and Antarctic Circumpolar Current (IO/ACC), Antarctic Circumpolar Current (ACC), Polar Front (PF), and mixed water of Polar Front and Fawn Trough (PF/Fawn Trough). **B**, Bacterial community structure of different water masses. Constrained Analysis of Principal Coordinates (CAP) of 16S rDNA diversity. OUT abundance table was used to calculate Bray- Curtis distances and constrained analysis was performed by water mass. Constrain reflects 58.5 % of overall variance in the data. There was a

significant relationship between water masses and community dissimilarity (adonis test; $p < 0.001$).
 Data with environmental samples represented as arrows. 30

Figure 16: Prokaryotic community composition of 3 samples each representing a water mass (Polar Front (PF), Antarctic Circumpolar Current (ACC) and Indian Ocean (IO)) as shown by 16S rDNA gene amplicon sequencing. All abundant phyla are shown as composite Krona plots (SilvaNGS) resolved down to the genus level. The relative fraction of Krona circles represents the relative abundance of kingdom, phyla, order, class, family, genus. Note that Chloroplasts and Mitochondria were not removed in this representation..... 16

Figure 17: Spearman correlation coefficients (r_s) plot including NO_3^- and NH_4^+ assimilation, C fixation and N_2 fixation rates as well as PSCs ($n=13$). For prokaryotic diversity, PSCs and chl *a* only T_0 samples were used for correlation calculations. Blue colour indicates positive correlation, red negative correlation. Cross indicates no significant correlation (significance level: $p = 0.05$). 16

APPENDIX FIGURES

Figure S- 1: gel after (A) 16S and (B) nifH amplicon PCR. A, 16S amplicon PCR. B, nifH amplicon PCR; PCR product was further used for Index PCR. Positive (+) and negative (-) controls worked for both PCR reactions..... 56

Figure S- 2: gel after (A) 16S and (B) nifH index PCR. negative controls (-) worked for both reactions, old PCR product used as positive control (+). 56

Figure S- 3: Mixed layer depth (MLD) and sea surface temperature (SST) (10m) for all sampling stations. A, MLD, showing deepest MLD in the PF around Kerguelen island. B, SST, showing clear temperature difference between IO and ACC..... 57

Figure S- 4: relative proportion of chl.a to total POC against SST..... 58

Figure S- 5: Distribution of sample sequencing depth of 16S amplicon sequence data..... 58

TABLES

Table 1: C fixation rates in different incubation bottles and Incubation bins (InT). Rep. 1, 3 and 5 were incubated in bin 1; Rep. 2, 4 and 6 were incubated in bin 2. Fixation rates in $\text{nmol C L}^{-1} \text{h}^{-1}$ 20

Table 2: Sampling stations visited during the OISO cruise, including N_2 fixation, ammonium and nitrate assimilation. NA indicates no data. Standard deviation (average \pm STD; $n = 3$ for stations 3, 9, 11, 15; $n = 6$ for stations E, 37, 2, 4, 6, 7, 14, 16, 18). 24

List of major abbreviations

ACC	Antarctic Circumpolar Current
Anammox	Anaerobic ammonium oxidation
AP	Accessory pigments
CTD	Conductivity temperature depth
DIC	Dissolved inorganic carbon
DIN	Dissolved inorganic nitrogen
DNA	Deoxyribonucleic acid
DO	Dissolved oxygen
HNLC	High nutrients low chlorophyll
IO	Indian Ocean
MIMS	Membrane Inlet Mass Spectrometry
MLD	Mixed layer depth
OISO	Océan Indien Service d'Observation
PF	Polar Front
PFT	Phytoplankton functional type
POC	Particulate organic carbon
PON	Particulate organic nitrogen
PSC	Phytoplankton size class
SO	Southern Ocean
SST	Sea surface temperature
TChla	Total chlorophyll a
TPig	Total pigments

1. Introduction

1.1 The Southern Indian Ocean and Southern Ocean

The Indian Ocean (IO) is an important contributor to global marine biodiversity and production of marine resources, yet is still the most understudied ocean worldwide (Wafar *et al.*, 2011; Alexander *et al.*, 2012; Hood *et al.*, 2016). The IO appears to be the most complex ocean regarding its topography and geology (Hood *et al.*, 2015). Topographic highs are important in terms of biodiversity for all trophic levels (Sheppard *et al.*, 2012; Boissin *et al.*, 2017; Sautya *et al.*, 2017). Different seabed depths and hydrothermal vents provide a variety of ecological zones (Sautya *et al.*, 2017) that are especially important for endemic species which are often rare and thus tend to be more vulnerable to climate change and pollution (Boissin *et al.*, 2017). Shallow platforms, like Chagos Archipelago, are refuges for fish and invertebrate larvae as well as a large coral reef area relatively undamaged by human interference (Sheppard *et al.*, 2012). Furthermore, topography impacts both ocean circulation and mixing, which can support unusually high productivity areas surrounded by less productive deep water (Hood *et al.*, 2015). However, biogeochemical processes in the warm oligotrophic waters of the southern Indian Ocean gyre remain poorly understood (Hood *et al.*, 2015).

In contrast to the oligotrophic waters of the IO gyre, the upwelled water of the Southern Ocean (SO) is comparatively nutrient-rich, meaning it consists of elevated sea surface concentrations of nitrate ($6 - 24 \mu\text{mol L}^{-1}$), phosphate ($0.4 - 1.6 \mu\text{mol L}^{-1}$) and silicic acid (up to $80 \mu\text{mol L}^{-1}$) (Levitus *et al.*, 1993). Large fractions of these upwelled waters are transported northwards to the warmer, saline waters of the polar front (PF). Eventually, they leave the surface through transformation into intermediate and mode waters (Wyrтки, 1973). Although these nutrient rich upwelled waters of the Southern Ocean are exposed to direct sunlight, phytoplankton growth is not widely stimulated, and chlorophyll *a* concentrations in the Southern Ocean generally remain lower than 1 mg m^{-3} (Boyd *et al.*, 2000). The low concentrations of iron (pico- nanomolar; Nolting *et al.*, 1998) in the open ocean limit the growth of phytoplankton and other microorganisms (Martin, 1992; Moore *et al.*, 2002). Therefore, these regions are described as high nutrient low chlorophyll (HNLC). Approximately 20% of the global ocean are HNLC regions (Goeyens *et al.*, 1998; Blain, Sarthou and Laan, 2008). The SO is the largest HNLC region in the world. However, massive phytoplankton

blooms occur regularly in the South Georgia, Crozet and Kerguelen regions (Sullivan *et al.*, 1993; Sarmiento *et al.*, 2004; Tyrrell *et al.*, 2005). The Kerguelen Islands and plateau sustain a distinct border, with warm, tropical water from the Indian Ocean to the north and the Subpolar Front to the south. The Kerguelen region is known for its high dissolved iron (DFe) concentrations ranging up to 0.51 nM DFe above the plateau in contrast to 0.09 nM DFe in the adjacent HNLC waters (Blain *et al.*, 2007; Bowie *et al.*, 2015). A strong vertical gradient in iron concentrations, ranging from 19 nM at the surface to maximum values of 0.51 nM close to the seafloor (Blain *et al.*, 2007), suggest a mainly sediment-derived contribution. High-energy internal tidal waves erode the sediment of the Kerguelen plateau and most likely cause such a vertical profile (Park *et al.*, 2008(a)).

1.2 The Nitrogen Cycle

Not only iron (Fe), but also other key nutrients such as nitrogen (N), shape the occurrence and abundance of phytoplankton and other organisms in the world ocean. Nitrogen serves both as building block (e.g. for deoxyribonucleic acid (DNA) and proteins), and as an energy source in catabolic reactions (Fig. 1). In seawater, nitrogen occurs mainly as dissolved di-nitrogen (N_2) gas. Most organisms cannot break the strong triple bond of N_2 and therefore rely on a reactive fixed form that is bonded to carbon, hydrogen, or oxygen (Fig. 1). Thus, fixed N can be a limiting factor for plankton biomass and growth in many marine ecosystems, such as the oligotrophic waters of the IO gyre and Pacific gyres.

To overcome this limitation, a group of microorganisms called diazotrophs have specialized to fix atmospheric N_2 into a usable form, thereby making themselves independent from dissolved and organic nitrogen (DON and PON) sources (Goering, Dugdale and Menzel, 1966). Diazotrophs are capable of breaking the triple bond of N_2 compound and converting it into organic N. This fixed N can be released through grazing pressure, bacterial interactions or environmental stress (Benavides *et al.*, 2013), which can then be taken up by other organisms such as phytoplankton. N_2 fixation is an important source of bioavailable N to marine waters and could possibly balance N losses through denitrification and anammox (Moore and Doney, 2007). Gruber and Sarmiento (1997) estimated global heterotrophic denitrification rates of $\sim 200\text{-}450 \text{ Tg N yr}^{-1}$. Rates for global N_2 fixation were estimated to be far lower, which are predicted to cause a significant imbalance of the global oceanic N budget (Gruber and

Galloway, 2008; Voss *et al.*, 2013). Recently, however, several model outputs indicate potential intense feedback loops between N_2 fixation, denitrification, and anammox that could maintain the global N budget in balance. N_2 fixation could be a crucial fixed N source, especially in oligotrophic environments like the subtropical gyres (e.g. the IO gyre) or marginal seas (Gruber and Sarmiento, 1997). It has also been estimated that N_2 fixation can support up to 50% of the primary production in tropical low productivity areas such as the eastern IO (Raes *et al.*, 2014). The quantity of N_2 fixation depends mainly on the sheer biomass of nitrogen fixing organisms, which in turn have an adaptive optima for temperature (Capone, 1997; Karl *et al.*, 2002; Staal, Meysman and Stal, 2003; Breitbarth *et al.*, 2007), iron (Falkowski, 1997; Kustka, Carpenter and Sanudo-Wilhelmy, 2002; Fu and Bell, 2003) and phosphorus availability (Karl *et al.*, 1997; Sañudo-Wilhelmy *et al.*, 2001; Moutin *et al.*, 2007). Studies revealed that even CO_2 concentration can influence growth rates and total biomass of diazotrophs (Levitan *et al.*, 2007; Hutchins *et al.*, 2015), thus raising the question whether increased pCO_2 concentrations (>400ppm; Tans and Keeling, 2018) would support global N_2 fixation. However, iron is mostly a limiting factor because it is an important co-factor of N_2 fixation (Falkowski, 1997; J. Kim and D. C. Rees, 1992; Raven, 1988).

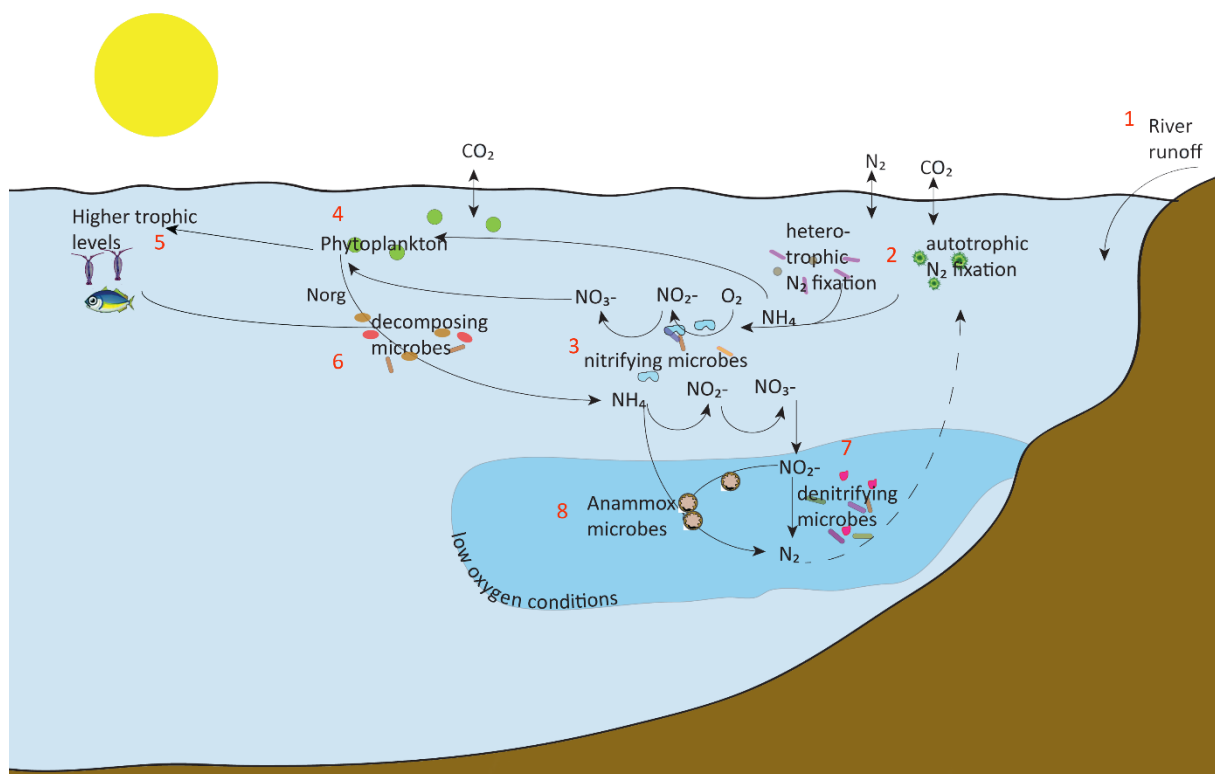


Figure 1: Marine nitrogen cycle. New nitrogen input from (1) river runoff and (2) autotrophic and heterotrophic nitrogen fixation. (3) Ammonium can be oxidized to nitrite and nitrate by nitrifying microbes. Ammonium and nitrate can be taken up by phytoplankton (4) and transferred to higher

trophic levels (5). Decomposing microbes can turn organic N (N_{org}) into Ammonium (6). Under suboxic conditions, nitrate can be reduced to Nitrite and N_2 by denitrifying microbes (7); Anammox (anoxic ammonium oxidation) microbes can oxidize ammonium using nitrite as electron acceptor to N_2 (8).

Physically different oceanic niches are occupied by different diazotrophic communities. The chain forming cyanobacterium *Trichodesmium* dominates warm, oligotrophic waters and contributes significantly to the global N budget (estimated to about $1.6-2.4 \cdot 10^{12}$ mol N yr^{-1} in the tropical North Atlantic; Capone et al., 2005). Besides *Trichodesmium*, the heterotrophic picoplankton UCYN-A (*Candidatus Atelocyanobacterium Thalassa*; Thompson et al., 2012) and *Crocospaera watsonii* have been postulated to have an equal or even higher contribution of N_2 fixation rates (Zehr et al., 2001; Montoya et al., 2004; Montoya, Voss and Capone, 2007; Großkopf et al., 2012; Martínez-Pérez et al., 2016). Furthermore, other diazotrophs occupy other adaptive zones than *Trichodesmium*, meaning that N_2 fixation regions outside the ecological optima of *Trichodesmium* have mostly been neglected so far. *nifH* gene analyses have revealed that UCYN-A occurs up to the edges of the Arctic and Antarctic circles (Moisander et al., 2010; Bentzon-Tilia et al., 2015; Messer et al., 2015; Scavotto et al., 2015; Fernández-Méndez et al., 2016; Martínez-Pérez et al., 2016). Moreover, the ability to fix nitrogen is not restricted to autotrophic organisms, but can also be detected in several heterotrophic prokaryotic clades, including Alpha- and Gammaproteobacteria as well as archaea (Mehta, Butterfield and Baross, 2003; Short, Jenkins and Zehr, 2004; Farnelid et al., 2011; Loescher et al., 2014).

The N cycle is closely interconnected with the C cycle through biological processes and the dependence of primary production on N availability. Oceanic phytoplankton contributes to around 50% of global net primary production (Field et al., 1998). Only 10% of the fixed C in the photic zone get eventually exported to the deep sea (Carbon pump), while 90% stays in the upper ocean through heterotrophic recycling processes (Michaels and Silver, 1988). Both the export of C and the recycling processes highly depend on the microbial community composition.

1.3 Aims of this Study

As a result of human-induced climate change and predicted increases in the thermal stratification of the oceans (Capotondi et al., 2012), the importance of N_2 fixation as a major N source for primary production has been brought to the focus of scientific attention (Hood, Coles and Capone, 2004; Breitbarth et al., 2007; Hood et al., 2015). Strong stratification

prevents nutrient fluxes across the pycnocline, meaning that primary productivity is limited by new nitrogen input (Boyd *et al.*, 2010; Garcia *et al.*, 2011). N_2 fixation can cause an excess of N in comparison to common N: P ratios (16; Redfield, (1958)) which is described by the N^* parameter ($N^*=[NO_3^-] - 16[HPO_4^{2-}]$; Gruber and Sarmiento, (1997)). We raise the importance of N_2 fixation as a major import source for new N and to balance N^* in the ocean. Physical factors, like temperature and mixed layer depth (MLD), as well as habitats and microbial community composition influencing the abundance of diazotrophs, will shift in the future. Even though the oligotrophic, warm waters of the Indian Ocean have been shown to provide a suitable environment for high N_2 fixation rates (Raes *et al.*, 2014; Waite *et al.*, 2013), very few studies have been conducted in the Southern Indian Ocean (González *et al.*, 2014). Our data, as part of the OISO (Ocean Indien Service d'Observation) campaign, contributes to a better understanding of the physical and biological factors controlling N_2 fixation in the Southern Indian Ocean and the French Southern and Antarctic lands during austral summer (January and February in 2017). Furthermore, this study sheds light on primary productivity and major N sources for autotrophic organisms in these waters. We expect that the distribution of water masses is a driving factor for physical and biological parameters. The cruise stations have been visited annually since 1997 and provide insights into long term nutrient availability. An in-depth understanding of biogeochemical and biological processes in this region will help to predict and model future scenarios in consideration of human induced climate change and pollution.

This study aims to investigate the differences in community composition as well carbon and N_2 fixation rates between different water masses. Our goal is to (1) describe the physical and biogeochemical conditions of the understudied area of the Southern Indian Ocean and the French Southern and Antarctic lands, spanning four different water masses. (2) to provide an in-depth understanding of the community composition of eukaryotic primary producers and prokaryotes. (3) to understand regional variations of carbon and N_2 fixation as well as ammonium and nitrate assimilation between four different water masses lastly, (4) to describe the occurrence of different diazotrophic organisms using diagnostic gene markers.

2. Materials and Methods

2.1 Sampling strategy

The Océan Indien Service d'Observation (OISO) MD206 cruise was conducted on board the R/V Marion Dufresne from 6th of January to 7th of February 2017 from La Reunion to the Kerguelen Islands in the Southern Ocean (49.25°S, 69.58°E) and back (Fig. 5 A). Stations covered an area from the Southern Indian Ocean Gyre to the Polar Front. Twenty stations were revisited as part of a larger repeated sampling campaign – OISO (<http://dx.doi.org/10.17600/17002400>). Physical and biogeochemical data as well as metadata from Conductivity Temperature Depth (CTD), starting in 1998, were evaluated, thereby allowing us to monitor changes in physical and chemical oceanographic properties over time. A combination of temperature, salinity and dissolved oxygen (DO) concentrations with dissolved inorganic nutrient concentrations (NO_3^- , NO_2^- , NH_4^+ , Si, and PO_4^{3-}) were assessed to characterize the physical and biogeochemical environment of the study region. Additional water samples from a flow-through intake (6m depth) were taken for dissolved inorganic nutrients (NO_x , NH_4^+).

During the MD206 voyage we conducted nitrogen fixation (N_2 fixation) and carbon fixation measurements, and nitrogen assimilation (NO_3^- and NH_4^+) measurements. Furthermore, we analysed the pelagic microbial community composition by means of distinct gene sequencing (16S, *nifH*) and pigment analysis. The 16S ribosomal DNA is a suitable primer to measure prokaryotic diversity. In contrast, the *nifH* gene is a functional gene of the nitrogenase and can therefore be used to assess diazotrophic diversity.

We measured temperature and oxygen throughout the water column. Seawater samples for dissolved inorganic carbon (DIC), silicate, NO_x and NH_4 were taken from Niskin bottles. Pigment analysis were performed using high performance liquid chromatography (HPLC; see below). N_2 and carbon fixation rates were obtained from incubation in bottles spiked with ^{15}N and ^{13}C on deck (see below). To be able to compare the interconnection between primary production, N fixation and assimilation, as well as the genetic signature of the microbial

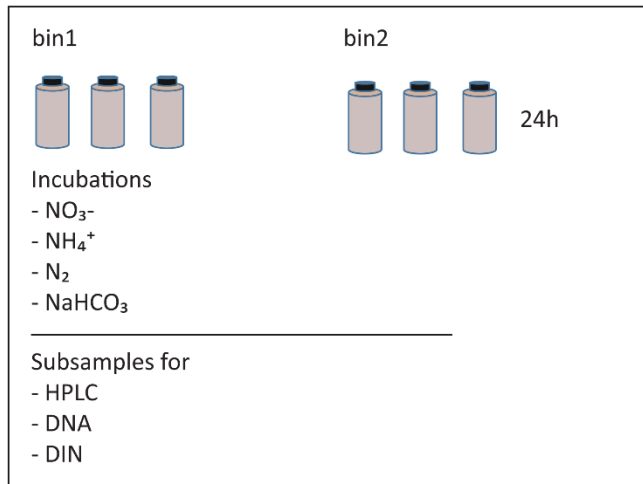


Figure 2: Schematic overview of experimental setup. Incubations were done in triplicates for each enrichment (NO_3^- , NH_4^+ , N_2 and NaHCO_3). TO as well subsamples from the incubations were taken for HPLC, DNA and DIN analysis in two different incubation bins

diversity, we conducted on-deck incubation perturbation experiments. Incubation bottles were incubated on board at ambient sea surface temperature (SST) using a flow through system (Fig. 3). We used two different incubation bins, which differed in their incubation temperature for certain stations (Fig.4). Temperature of both incubation bins was continuously measured (Fig. 4). We used a neutral density screen to correct for incident light intensity.

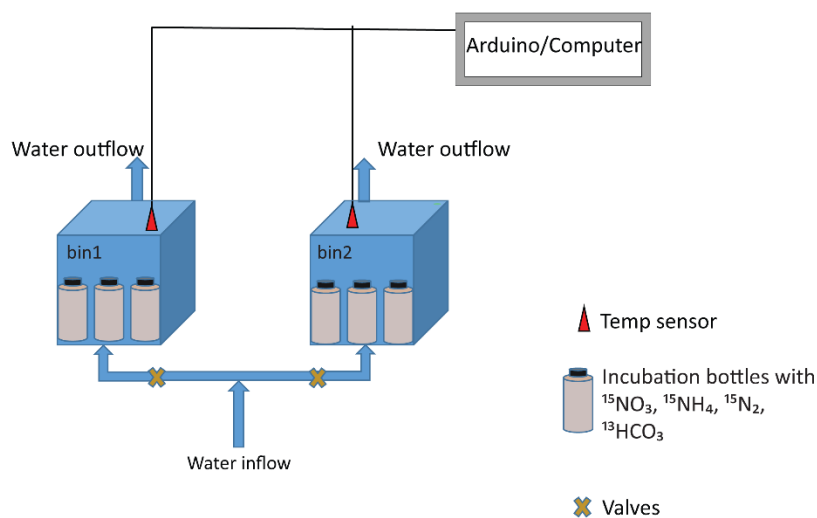


Figure 3: Schematic of incubation setup. Water inflow from ship underway system. Arduino continuously measured temperature in both bins.

2.2 Perturbation experiments

The temperature of the incubation bins was unexpectedly high with respect to *in situ* sampling temperatures (Fig. 4). Moreover, variations within one incubation bin ranged up to $\Delta 20^{\circ}\text{C}$ on a time range over 24 hours (Station 4). Overall, the difference between bin 1 and bin 2 was significant (paired t-test; $p < 0.002$, $n = 26307$) with a mean differences of 1.02°C . Both bin 1 and bin 2 were significantly different from the in-situ temperature with a mean difference ($n = 14$) of 5.6°C and 4.6°C , respectively.

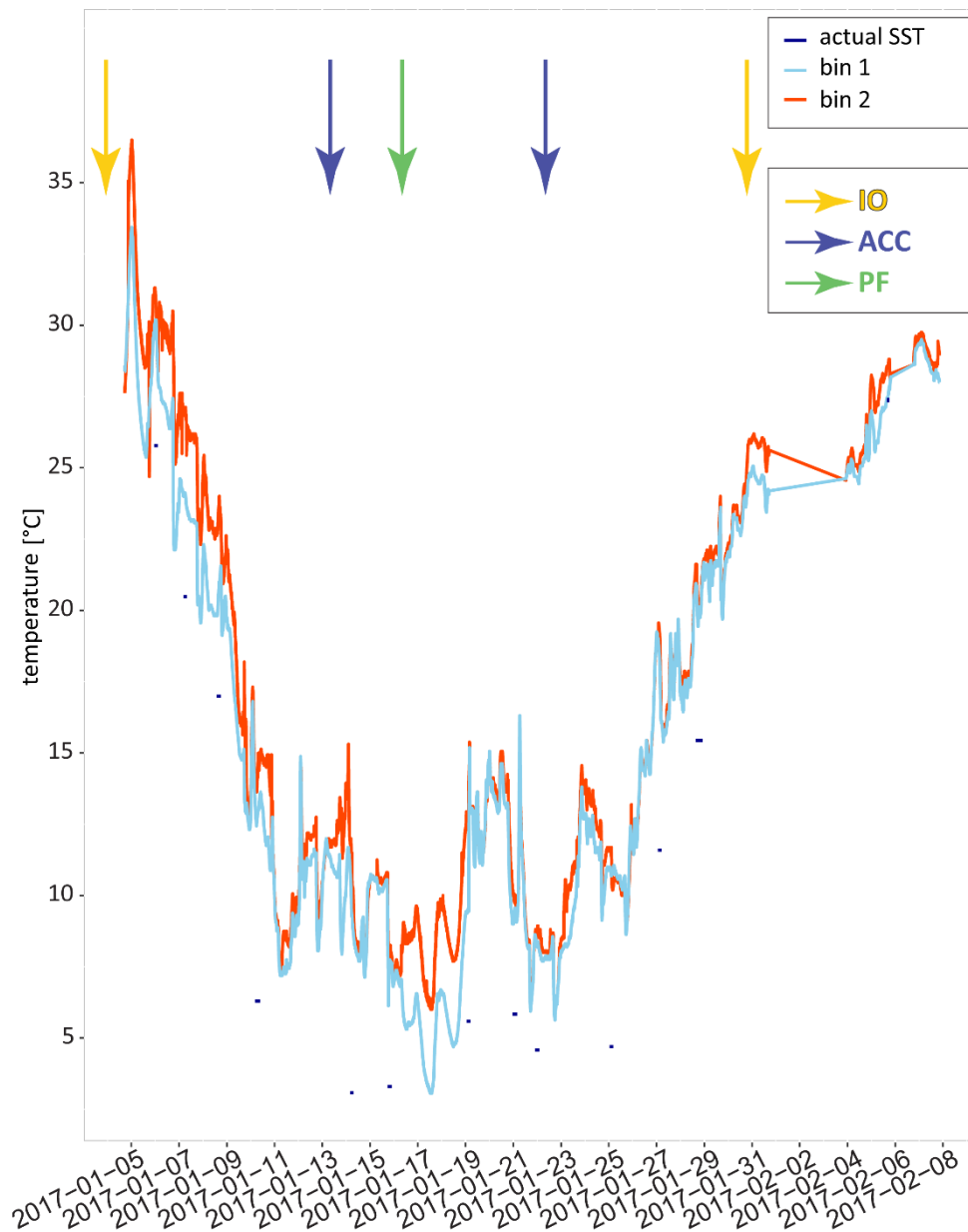


Figure 4: Temperature continuously measured in incubation bins (blue line bin 1, red line bin 2) and sporadically for sea surface temperature (SST) (black dots). Arrows indicate where ship was crossing different fronts; yellow arrows highlight Indian Ocean (IO), blue arrows indicate Antarctic circumpolar current (ACC) and green arrow highlights polar front (PF)

2.3 Biophysical data

Salinity, temperature and oxygen data were collected at each station using a 24- Niskin bottle rosette with a Seabird SBE32 conductivity- temperature- depth (CTD) system equipped with a SBE43 O₂ sensor and a Chelsea Aqua tracker fluorometer.

Mixed layer depth was calculated using $\Delta d = 0.03 \text{ kg m}^{-3}$ compared to a surface reference depth of 5 m according to Thomson and Fine (2003).

2.4 Nutrient Analysis

Dissolved inorganic nutrient concentrations, including phosphate (PO₄³⁻), silicate (Si(OH)₄), mono- nitrogen oxides (NO_x), nitrite (NO₂⁻) and ammonium (NH₄⁺) were assayed on a Quattro39 Continuous Segmented Flow Analyzer (Seal Analytical). Calibrations were conducted using potassium dihydrogen phosphate for PO₄³⁻, sodium meta-silicate nonahydrate for Si(OH)₄, potassium nitrate for NO_x, sodium nitrite for NO₂⁻ and ammonium sulphate for NH₄⁺. All calibrations were corrected for concentrations using certified reference materials (CRM) CRM1 CJ-2050 (target conc. 16.67 μmol L⁻¹) and CRM2 CD-0342 (target conc. 5.65 μmol L⁻¹). Calibration curves had an R² value of 0.999. Phosphate, silicate, mono-nitrogen oxides and nitrite were measured following widely used colorimetric methods (Armstrong, 1951; Murphy and Riley, 1962; Wood, Armstrong and Richards, 1967) with adaptations to particular needs for Seal Analytical QuAAtro autoanalyzer (*unpublished*). Phosphate, molybdate ion and antimony ion follows a reduction with ascorbic acid to a blue phospho-molybdenum complex that can be read at 880 nm. The detection limit of phosphate with this method is 0.01 μmol L⁻¹. The detection of silicate is based on the reduction of a silicomolybdate complex in acid solution to molybdenum blue by ascorbic acid. The absorbance is measured at 820 nm (detection limit: 0.3 μg L⁻¹). Determination of nitrate and nitrite is based on the reduction of nitrate to nitrite at pH 8 in a copperized cadmium reduction coil. Nitrite reacts under acid conditions with sulphanilamide to a diazo compound which couples with N-1-naphthylethylenediamine dihydrochloride (NEDD) to form a reddish-purple azo dye. The absorbance is measured at 520nm (detection limit 0.03 μmol L⁻¹). Nitrite concentration is measured the same way without the previous reduction step from nitrate to nitrite (detection limit 0.01 μmol L⁻¹).

Ammonium was measured using a fluometric method (Keroul et al. 1997). The sample reacts with o-phthalaldehyde (OPA) at 75°C in the presence of borate buffer and sodium sulfite to

form a fluorescent species proportional to the ammonia concentration. The fluorescence was measured at 460 nm following excitation at 370 nm.

2.5 Functional pigment analysis

For HPLC analysis, 4 L of seawater were filtered (< 10 kPa) on 47 mm Whatman GF/F filter and stored at -80°C until further analysis. Samples were dissolved in 4 ml acetone and disrupted using glass beads and included 150 µl of the internal standard canthaxanthin. Detection of the sample at 440 nm absorbance using a HPLC analyser (VARI AN Microsorb- MV 100-3 C8). Pigment concentration were calculated according to Kiliyas et al. (2013).

HPLC output data were analysed using diagnostic pigments for the different taxa after Hirata et al. (2011). Furthermore, diagnostic pigments were used to delineate three different size classes (pico-, nano-, and microplankton) according to Vidussi et al. (2001). Relative proportion of each phytoplankton size class (PSC) was calculated using a linear regression model proposed by Uitz et al. (2006). The relative proportion of phytoplankton functional types (PFTs) to the sum of diagnostic pigments was calculated after Hirata et al. (2011). We checked for ultraoligotrophic conditions ($\text{chl } a < 0.08 \text{ mg m}^{-3}$; Brewin et al., 2010), however, none of our stations was ultraoligotrophic according to these terms. Pigment data were quality controlled after these three statistical rules according to Aiken et al. (2009):

(1) The difference of total chlorophyll a (TChl a) and accessory pigments (AP) must be less than 30% of the total pigment concentration (TPig concentration).

(2) The regression between TChl a and AP should have a slope within the range of 0.7 - 1.4 and a $R^2 > 0.9$.

(3) the data can be accepted only if > 85% of the dataset passes the first two rules.

For our data, the difference between TChl a and AP varied in the given range between 7% and 27%, with one outlier in OISO 37 (51%) because of the high quantification of diatoxanthin (and beta carotenoids). The regression between TChl a and accessory pigments had a slope of 0.96 and $R^2 > 0.9$.

Supplementary data are available at <https://doi.pangaea.de/10.1594/PANGAEA.885895> (*DOI registration in progress*).

2.6 Microbial diversity analysis based on 16S rDNA

Two litres of seawater from each station were filtered through a 0.22 µm Sterivex® filter cartridge for DNA isolation, snap frozen in liquid nitrogen and stored at -80°C until extraction at the shore-based laboratory.

DNA was extracted using a DNeasy® Plant Mini Kit (QIAGEN, Valencia, CA, USA, Catalog No./ID: 69106) following the manufacturer's instruction with some modifications for cell disruption. Sterivex cartridges were gently cracked open and filters were removed and transferred into a new and sterile screw cap tube. Approximately 0.3 g of pre-combusted glass beads (Ødiameter 0.1 mm; 11079101 Bio Spec Products) and 400 µl Buffer AP1 were added to the filter, followed by a bead beating step with two times at 5500 rpm for 20 seconds with two minutes on ice in between and a final beat beating step at 5000 rpm for 15 seconds.

After DNA extraction, DNA concentration was quantified by the Quantus™ Fluorometer and normalized to 2 ng µl⁻¹.

2.6.1 Amplicon 16S PCR

To determine the bacterial community composition, we amplified the v4 and v5 hypervariable regions of the 16S gene using universal primers proposed by Parada et al. (2016). DNA amplification was conducted in a triplicate 22µl reaction mixture containing 8 ng DNA, 4 µl of 1 µM forward primer 515F-Y (5'-GTG YCA GCM GCC GCG GTA A-3'), 4µl of 1µM reverse primer 926R (5'-CCG YCA ATT YMT TTR AGT TT-3') and 10 µl 2x KAPA HiFi HotStart ReadyMix (Roche). Cycling conditions included a 5min heating step at 95°C followed by 25 cycles of 95°C for 45 s, 60°C for 45 s and 72°C for 30 s. Triplicate reactions were pooled, and 5 µl were used to check for amplification on a 1% agarose gel using 5x Gel pilot loading dye (Qiagen).

The second amplification procedure was performed as described above, but the annealing temperature was at 65°C and the cycle number was reduced to 10 cycles. 1 µl of the product was used as template for index PCR to a total volume of 12 µl reaction volume using 1 µl primer (bioosystems' 384 12-base barcodes), 4 µl PCR water and 6 µl NEBNext Q5 Hot Start HiFi PCR Master Mix (New England Biolabs). The PCR product was checked on a 1% agarose gel (see appendix Fig. S-1). 3 µL from each reaction were pooled and purified using QIAquick PCR Purification Kit (QIAGEN, Valencia, CA, USA).

2.6.2 Amplicon nifH PCR

To determine diazotrophic diversity, we amplified the *nifH* gene using universal primers nifH1-4 (eurofins Genomics, Germany) in a nested polymerase chain reaction (PCR; Zehr et al., 2001; Zehr and McCreynolds, 1989). In the first step of the nested PCR we used forward primer nifH4 (5'-TTYTAYGGNAARGGNGG-3') and reverse primer nifH3 (5'-ATRTTRTTNGCNGCRTA-3'). In the second PCR nifH1 (5'-TGYGAYCCNAARGCNGA-3') and reverse primer nifH2 (5'-ADNGCCATCATYTCNCC-3') were used. For the third PCR, specific overhang adaptors were attached to the nifH1 and nifH2 primers. We used cultivated *Clostridium pasteurianum* as a positive control. DNA amplification was done in duplicate, with 25 µl total reaction volume containing 10ng DNA template, 4 µl of 10 µM forward primer and 4 µl of 10 µM reverse primer and 12 µl 2x KAPA HiFi HotStart ReadyMix (Roche). Cycling conditions were followed after Gradoville et al. (2017). The reaction was cycled at 94°C for 7 min followed by 30 cycles of 94°C for 1 min, annealing at 57°C for 1 min, and extension at 72°C for 1 min, with a final extension at 72°C for 7 min. The second round of *nifH* PCR was with the same thermocycling conditions and components but 1 µL PCR product from the first reaction was used as a template for the reaction mixture. 10 µl of reaction product was checked on a 1% agarose gel with Qiagen Gel Pilot 5x loading dye (Appendix Fig. 1). PCR product was cleaned using AmPure XP beads following the protocol for 16S Metagenomic Sequencing Library Preparation.

2.6.3 Index PCR

To add the Illumina-specific adapters and sample specific barcodes, we used 1 µl of previous PCR product to a total volume of 12 µl, including 1 µl primer (12bp barcode and Illumina adapter 384; applied biosystems), 4 µl PCR grade water and 6 µl Mastermix (NEBNext Q5 Hot Start HiFi PCR Master mix). The reaction was cycled at 95°C for 5 min, followed by 15 cycles of 95°C for 45 sec, annealing at 60°C for 20 sec, and extension at 72°C for 30 sec. PCR product was checked on a gel (Appendix Fig. S-2). 3 µl of each sample were pooled and cleaned with QIAquick PCR Purification Kit (Qiagen). DNA concentration was quantified with Qubit™ dsDNA HS Assay Kit (ThermoFisher).

2.6.4 Sequencing and data analysis

PCR products were sequenced using MiSeq Sequencer (Illumina) at EMBL in Heidelberg (Germany). Nucleic acid sequence data were trimmed using Trimmomatic (Bolger, Lohse and Usadel, 2014). Paired end reads were merged using PEAR (Zhang *et al.*, 2014). We used

Cutadapt (Martin, 2011) to adjust read direction (forward primer- read- reverse primer) and to cut primers. We filtered for reads based on phred scores with an expected error of ± 50 bp read length difference and denovo chimeras (vsearch; Rognes et al., (2016)). Sequence reads were clustered to operational taxonomic units (OTUs) using swarm (Mahé *et al.*, 2014). OTU singeltons were removed. We used the software mothur[®] for taxonomical annotation having Silva database as reference data for 16S amplicon data. All *nifH* amplicons were annotated using diazotroph database by Luo et al. (2012). For statistical analysis, we removed Chloroplast and Mitochondria from 16S dataset since they are no true representatives of the bacterial community.

Further, we analysed taxonomic diversity in our samples using SILVAngs (<https://www.arb-silva.de/ngs/Index.html#>). SILVAngs is an automated data analysis service for 16S or 18S rDNA amplicon reads from high-throughput sequencing. Therefore, the SILVA rDNA database and taxonomies are used as a reference.

Here, we only present 16S sequence data since *nifH* data analysis has not been completed yet.

2.7 N₂ fixation rates

N₂ fixation experiments were carried out in triplicates for each station. Incubations were executed in acid-washed polycarbonate bottles on deck with ambient light conditions. All polycarbonate incubation bottles were rinsed with deionized water and seawater prior to incubation. We used the combination of the bubble approach (Montoya *et al.*, 1996) and the dissolution method (Mohr *et al.*, 2010) proposed by Klawonn et al. (2015). Bottles were filled up headspace-free. Incubations were initialized by adding a 10 ml ⁻¹⁵N₂ gas bubble. Bottles were gently rocked for 15 minutes. Finally, the remaining bubble was removed to avoid further equilibration between gas and the aqueous phase. After 24 hours, a water subsample was transferred to a 12 ml exetainer and preserved with 100 µl HgCl₂ solution for later determination of exact ¹⁵N-¹⁵N concentration in solution. Natural ¹⁵N₂ was determined using Membrane Inlet Mass Spectrometry (MIMS; GAM200, IPI) for each station. MIMS is a highly precise method to determine N₂ isotopes (²⁸N₂, ²⁹N₂, ³⁰N₂). Calibration of the system was done with air saturated water (salinity = 0 psu).

Bottles were incubated in triplicates for 24 hours in one of the two incubation bins (bin 1 or bin 2). N₂ fixation experiments were terminated by collecting the suspended particles from each bottle by gentle vacuum filtration through a 25 mm pre-combusted GF/F filter (pressure drop <10 kPa) immediately after enrichment (T₀) and 24 hours (T₂₄). Filters were snap frozen in liquid nitrogen and stored at -80°C while at sea. Filters with enriched and T₀ samples were acidified and dried overnight at 60°C. Analysis of ¹⁵N₂ incorporated was carried out by the Isotopic Laboratory at the UC Davis, California campus. The detection limit for δ¹³C is 0.2 ‰ and 0.3 ‰ for δ¹⁵N.

We calculated nitrogen fixation rates after Montoya et al. (1996) with the exception that rates are displayed in nmol N L⁻¹ d⁻¹.

$$N \text{ uptake } [nmol N L^{-1} d^{-1}] = \frac{PN_{enriched}[nmol L^{-1}] * (\delta_{enriched} - NA)}{(\delta_{initial} - NA) * d} \quad (1)$$

Supplementary data are available at <https://doi.pangaea.de/10.1594/PANGAEA.885894> (*DOI registration in progress*). Furthermore, we calculated the minimum quantifiable rate according to Montoya et al. (1996) and Gradoville et al. (2017). The minimum quantifiable rate is the square root of the total variance, meaning the sum of all possible error contribution calculated of the variance between all replicates for PN_{final}, PN_{initial} and PON. Supplementary data are available at <https://doi.pangaea.de/10.1594/PANGAEA.885932> (*DOI registration in progress*).

2.8 Carbon and Nitrogen assimilation experiments

We used stable isotope tracers (¹⁵N) to measure dissolved inorganic nitrogen (DIN) assimilation rates. Experiments were initiated by adding a known concentration of 0.05 of K¹⁵NO₃ and ¹⁵NH₄Cl for oligotrophic waters of the IO and 0.625 μmol L⁻¹ for HNLC regions in the ACC and PF (Knap et al., 1994, Waite et al., 2007) to one litre polycarbonate bottles. For the incubation, we followed the same procedure as for N₂ fixation experiments. In order to obtain the natural abundance of PON/C, which is needed as a t-zero value to calculate the assimilation rates, 4 L of water were filtered onto a pre-combusted GF/F filter for each station. Carbon assimilation rates were calculated according to Knap et al. (1996).

$$C \text{ uptake } [nmol C L^{-1} h^{-1}] = \frac{(C_{enriched} - NA) * POC_{enriched}}{\left[\frac{100 * 13C}{13C + 12C} \right] - NA} * h \quad (2)$$

Additionally, we normalized the ^{13}C assimilation rates for carbon fixation efficiency with biomass obtained from HPLC data using the total volume of pigments.

$$C \text{ uptake } [\mu\text{mol C g}^{-1} \text{ h}^{-1}] = \frac{C \text{ uptake } [\text{nmol N L}^{-1} \text{ h}^{-1}]}{\text{Biomass } [\text{ng} \cdot \text{L}^{-1}]} \quad (3)$$

Nitrate and Ammonium assimilation rates were calculated according to Knap et al. (1996).

$$\text{NO}_3 \text{ uptake } [\text{nmol N L}^{-1} \text{ d}^{-1}] = \frac{(\text{NO}_3\text{-enriched} - \text{NA}) * \text{PN}_{\text{enriched}}}{\left[\left[\frac{100 * 15\text{N}}{15\text{N} + 14\text{N}} \right] - \text{NA} \right] * d} \quad (4)$$

$$\text{NH}_4 \text{ uptake } [\text{nmol N L}^{-1} \text{ d}^{-1}] = \frac{(\text{NH}_4^+\text{enriched} - \text{NA}) * \text{PN}_{\text{enriched}}}{\left[\left[\frac{100 * 15\text{N}}{15\text{N} + 14\text{N}} \right] - \text{NA} \right] * d} \quad (5)$$

Supplementary data are available at <https://doi.pangaea.de/10.1594/PANGAEA.885892> (DOI registration in progress).

2.9 Statistical analysis

All statistical tests were performed in R version 3.3.3 (R Core Team, 2017). Differences in temperature were analysed using paired t-test between both bins and between bins and in situ temperature, respectively. Relationships between nutrient distribution and assimilation rates were tested for correlation with latitude, salinity and sea surface temperature (SST). For most of the data (except N_2 fixation rates, where salinity could explain more of the variance) SST had the best fit. In the following we only show correlation plots against SST.

Nutrient (NO_3^- , PO_4^- , Si) and DIC concentrations could be described using a trendline (4th polynomial fit) and tested for significance using linear regression. C and N_2 fixation, as well as NO_3^- and NH_4^+ assimilation rates were tested for significant relationships with SST using linear regression model. Trendlines for absolute C fixation was tested for significance using a linear regression model. Differences between incubations in bin 1 and bin 2 were tested using a paired t-test. Differences in community composition, using pigment concentrations, in bin 1 and 2 and between stations were analysed using two-way ANOVA. Two-way ANOVA was also used assessing differences in total biomass in bin 1 and 2 and between stations. Phytoplankton size classes (PSCs) relative abundance followed 2nd polynomial fits which were tested for significance using linear regression models.

Autotrophic community composition analysis was performed using the concentrations of the HPLC analysis using the packages phyloseq and vegan. Principal coordinate analysis (PCoA) was calculated based on Bray- Curtis dissimilarity matrix. Significant differences between water masses were analysed using Adonis test (vegan package) along with a beta dispersion test to evaluate the homogeneity of dispersion. To see how environmental variables are associated with the different sites, we used a constrained ordination to linear combinations of the environmental parameters. We combined the environmental scores with the unconstrained analysis of the HPLC analysis data. We checked the constrained ordination axes for significance using permutational ANOVA, which was significant ($Pr(>F) = 0.001$).

DNA analysis was performed using the package phyloseq. Distribution of sample sequencing depth was visualized, to examine a normal distribution of the reads (appendix Fig. S-5) Relative abundance of phyla (>2%) were calculated and plotted. Unconstrained ordination analysis, using the function from miseqR.R for scaling the data. Principal coordinate analysis (PCoA) and non-metric dimensional scaling (NMDS) were calculated based on Bray- Curtis dissimilarity matrix. In case of NMDS, a square root transformation and Wisconsin double standardization were performed prior to analysis. Significant differences between water masses were analysed using Adonis test (vegan package) along with a beta dispersion test to evaluate the homogeneity of dispersion. To see how environmental variables are associated with the different sites, we used a constrained ordination to linear combinations of the environmental parameters. We combined the environmental scores with the unconstrained analysis of the OTU table. We checked the constrained ordination axes for significance using permutational ANOVA, which was significant ($Pr(>F) = 0.001$).

We calculated Richness and alpha diversity (Inverse Simpson Index) in each sample by subsampling the minimum number of reads (9246) to estimate the species abundance of the real population. We repeated the calculation 100 times and averaged the results from all trials to achieve best estimate of real diversity by standardizing the sampling effort.

Correlations between all physical (Salinity, Temperature, MLD), nutrients (NH_4^+ , NO_x , PO_4^- , Si), PSCs as well as assimilation rates were tested for significant relationships using spearman correlation.

3. Results

3.1 Hydrographic conditions

The OISO MD206 cruise took place in the Austral summer in the south Indian Ocean and Subpolar region around Kerguelen island. The study site is characterized by three major water masses, namely the Southern Indian Ocean Gyre (IO), the Antarctic Circumpolar Current (ACC) and the Polar front (PF), which is partly influenced by the Fawn Trough (Fig. 5 A; combined from Park *et al.*, 2008(b)). These water masses separate physically according to their salinity and temperature values (Fig. 5 B). The Indian Ocean Gyre is characterized by warm (20-25°C), saline (>35psu) water. The ACC is distinct from the IO according to surface temperature (3-6°C) and salinity (<34psu). The PF is more saline than the ACC (~33.8 psu) while sea surface temperature is around 4.7°C ±0.1°C. Depth profiles for temperature, oxygen and salinity along two longitudinal transects indicate a clear difference between IO and ACC (Fig. 6). The first transect covers OISO stations 2, 3, 4, 6, and 37 (30°S – 50°S Latitude, 53 ± 0.9 °E Longitude; mean ± SD; Fig. 6 A-C). The second transect, located further east, covers the stations 18, 16, 15, 14, E, 10, 11 (27°S – 56°S Latitude, 70 ± 5°E Longitude; mean ± SD; Fig. 6 D-E). Both transects show significant decrease in temperature and salinity and increase in oxygen concentration crossing from the IO to the ACC. The difference between ACC and PF, however, is not as distinct as the IO and ACC.

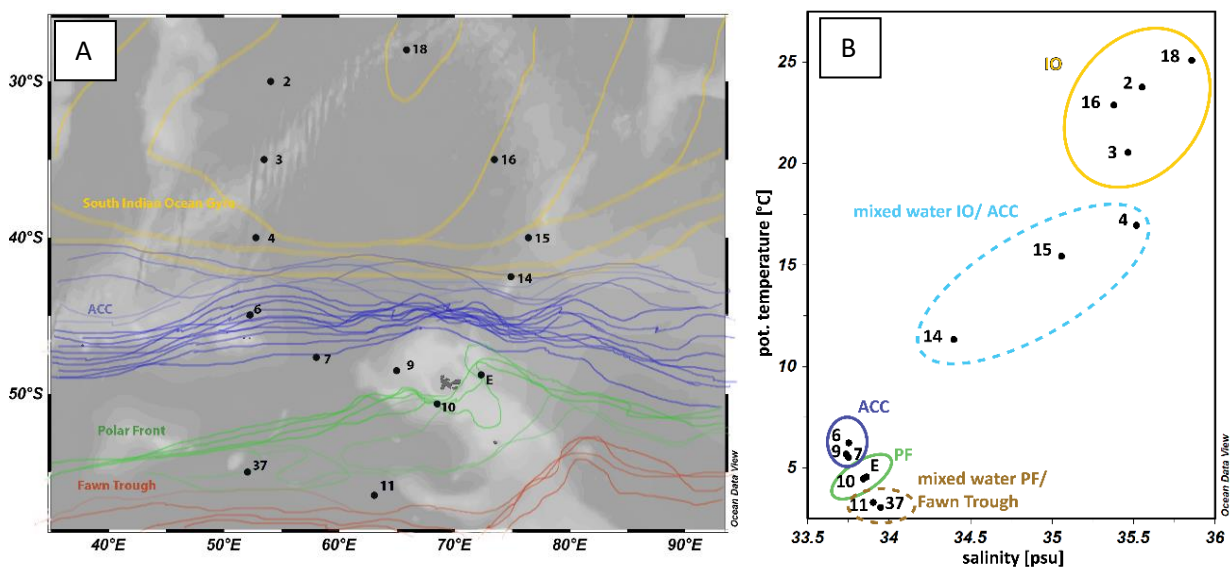


Figure 5: A, Map of sampling stations within different water masses, water masses modified from Park *et al.* 2008(b); B, Temperature- salinity plot differentiating these water masses. Mixed water is encircled with dashed lines.

The mixed layer depth (MLD) showed high variability among the stations (appendix Fig. S-3). MLD was deepest above the plateau (82 – 91 m; Station 10, E) and shallowest in the IO (<23 m; Station 2,3,16,18).

The Kerguelen plateau is characterized by natural iron fertilization (Station E; Blain et al., 2007) while off the plateau (Station 37,11) high nutrient low chlorophyll (HNLC) conditions prevail (Hart, 1942; Sullivan *et al.*, 1993; Tyrrell *et al.*, 2005; Blain *et al.*, 2007).

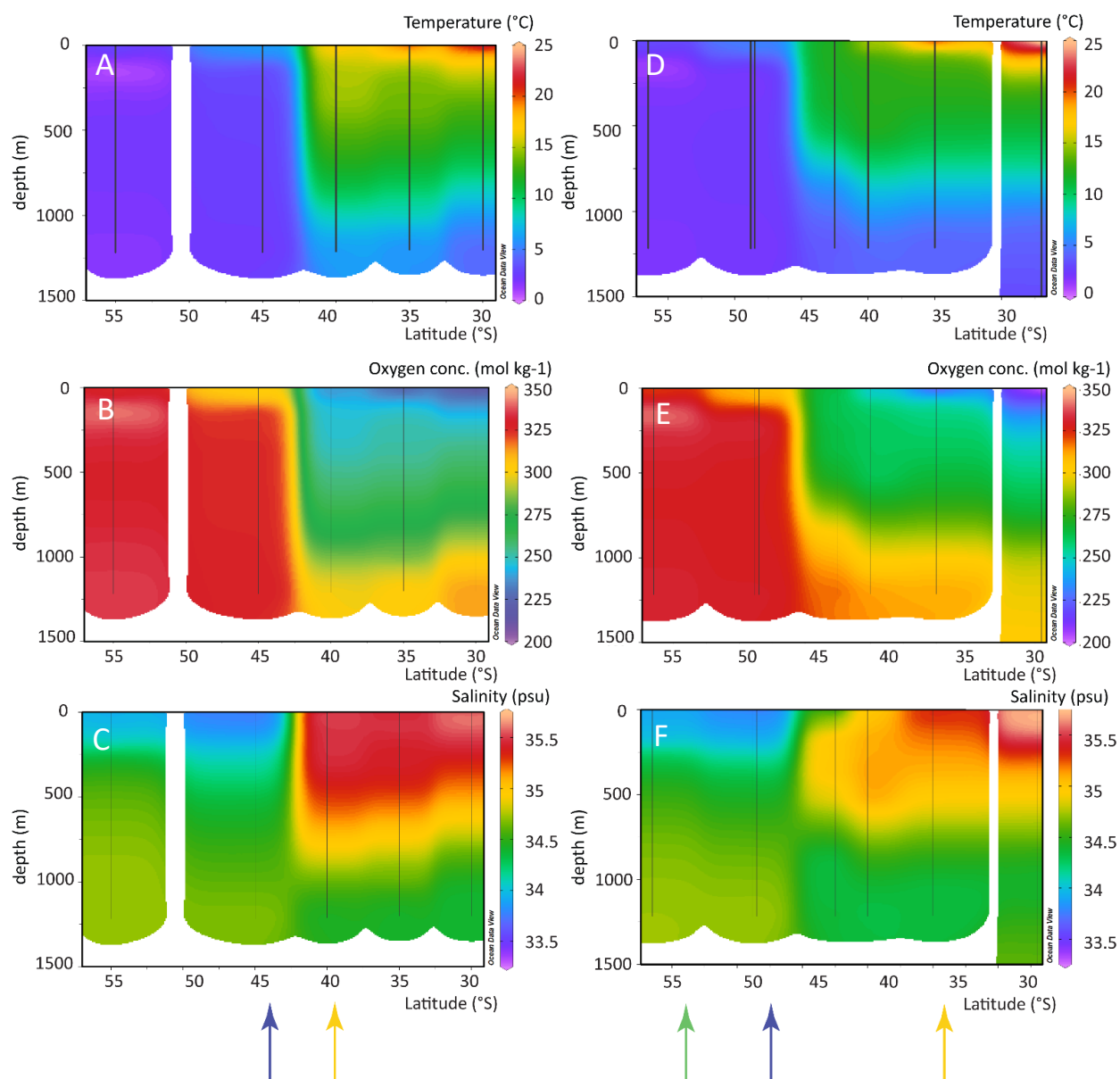


Figure 6: Depth profiles of temperature, oxygen and salinity along two transects of the OISO stations. **A-C**, covering OISO stations 2, 3, 6 and 37; a clear difference in all parameters is shown between IO and ACC. **D-F**, show latitudinal transect of OISO stations E. Blue arrows highlight the Antarctic circumpolar current (ACC), green arrow the Polar Front (PF) and yellow arrows the Indian Ocean (IO).

3.2 Nutrient distributions

Nutrient concentrations were regularly measured around the same time of the year (January-February) as part of the OISO campaign. Nitrate concentrations increased with decreasing SST (Fig. 7 A). The solubility of NO_3^- follows an exponential decrease with increasing temperature (trendline 4th polynomial fit; $R^2 = 0.91$, $p < 0.002$, $n = 81$). In warmer surface waters of the Indian Ocean (IO) nitrate concentration was below detection limit. Phosphate concentrations follow a similar trend as nitrate (Fig. 7 B; $R^2 = 0.93$, $p < 0.001$, $n = 19$). N^* ($[\text{NO}_3^-] - 16[\text{PO}_4^-]$; Gruber and Sarmiento, (1997)) varies between -1.5 and -3.6 in cold-water in cold water ($<15^\circ\text{C}$ SST), which is slightly less than the Redfield ratio (16N:1P; Redfield, 1958). For the warm water stations ($>15^\circ\text{C}$ SST), however, N^* could not be calculated because N concentrations were below the detection limit. Silicate concentrations remained low down to 5°C SST and then exponentially increased (trendline 4th polynomial fit; $R^2 = 0.67$, $p < 0.002$, $n = 88$). Maxima of Si concentrations were measured in the mixed water of the PF and Fawn Trough with concentrations of 20 and $25 \mu\text{mol kg}^{-1}$ (Station 11, 37). Dissolved inorganic carbon (DIC) concentrations changes not only between temperatures but also over time. DIC concentration follows a 4th order polynomial regression ($R^2 = 0.81$, $p < 0.002$, $n = 62$) with a decline in concentration towards higher temperature according to its solubility. However, a local maximum around 20°C SST is shown (Fig. 7 D). The DIC concentration increased over the past 19 years, having an increase of an average of $34 \pm 10 \mu\text{mol kg}^{-1}$ between 1998 and 2017.

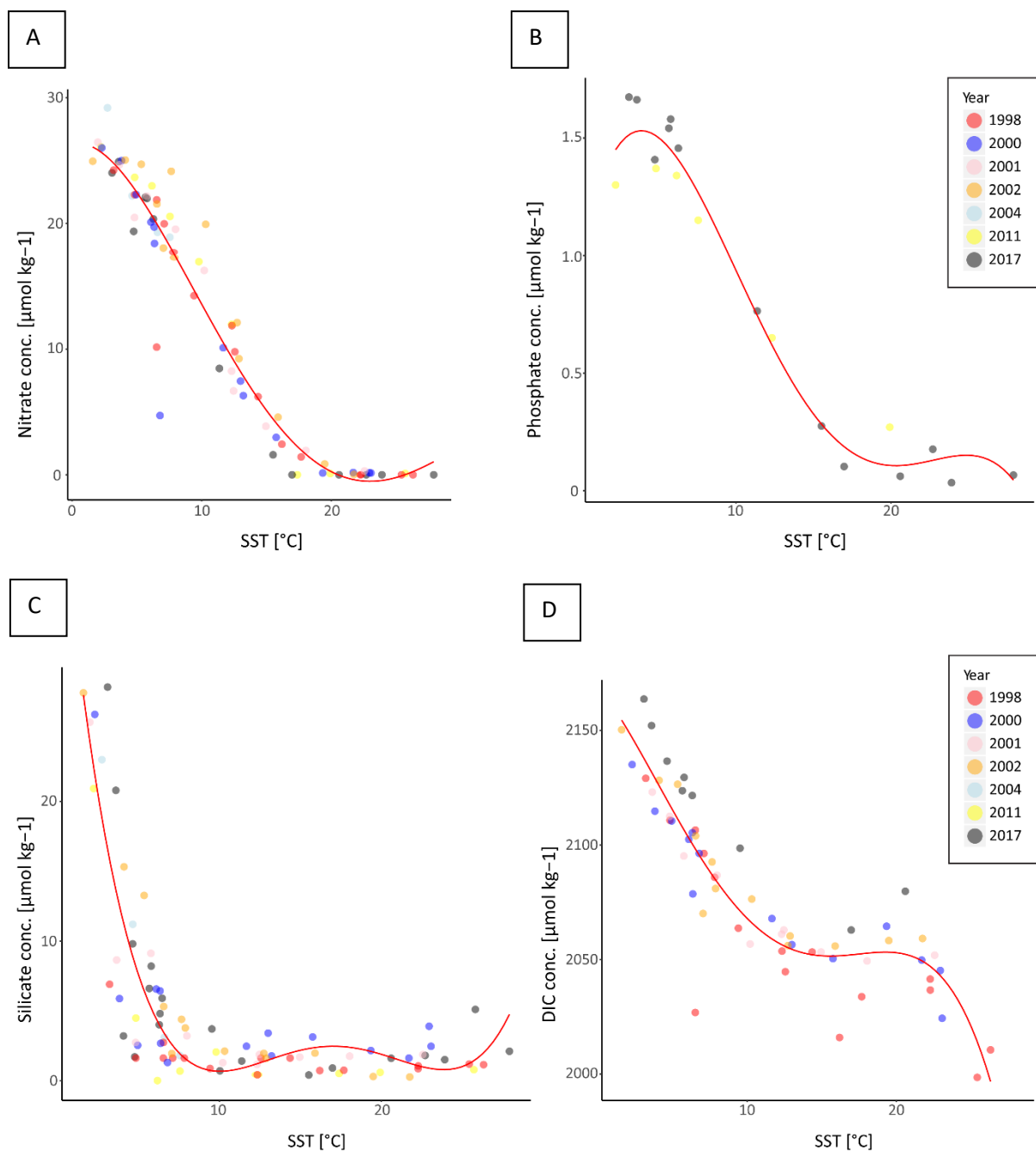


Figure 7: Nutrient and DIC concentration against sea surface temperature (SST) over the past 19 years. Trendlines 4th polynomial fit. **A**, nitrate concentration in $\mu\text{mol L}^{-1}$. **B**, phosphate concentration in $\mu\text{mol L}^{-1}$. **C**, Silicate concentration in $\mu\text{mol L}^{-1}$. **D**, DIC concentration in $\mu\text{mol kg}^{-1}$.

3.3 Carbon and Nitrogen fixation rates

Total ^{13}C assimilation was highest at Station 9 (141.5 $\text{nmol L}^{-1} \text{h}^{-1}$) and Station E (111 $\text{nmol L}^{-1} \text{h}^{-1}$), both above the Kerguelen plateau. High ^{13}C assimilation rates were also measured in other stations of the ACC (Stations 6, 7) and mixed water between IO and ACC (Stations 4, 14, 15). Lowest uptake rates were measured for IO stations with a maximum of 26.8 $\text{nmol L}^{-1} \text{h}^{-1}$ (Station 3). Overall, a maximum was reached in the mixed water of the IO and ACC, dropping on either side of the front, both towards warmer and colder water (Fig. 8 A; $p < 0.001$, $R^2 = 0.52$, $n = 65$). While warm-water stations show very little variations within one station (e.g. $12.6 \pm 2.5 \text{ nmol L}^{-1} \text{h}^{-1}$, mean \pm SD, $n = 6$, Station 18) and water mass, variation within cold-water stations was relatively high (e.g. $49.4 \pm 23.5 \text{ nmol L}^{-1} \text{h}^{-1}$, mean \pm SD, $n = 6$, Station 37). Biomass-specific ^{13}C uptake showed a different scenario relative to absolute fixation values. In this case, average rates in the IO were highest (93.2 $\mu\text{mol kg}^{-1} \text{h}^{-1}$). The maximum rate was still at Station 9 (170.59 $\mu\text{mol kg}^{-1} \text{h}^{-1}$), but other stations in the ACC had very low carbon uptake efficiency (44.7 $\mu\text{mol kg}^{-1} \text{h}^{-1}$, Station 6 bin 1; 58.31 $\mu\text{mol kg}^{-1} \text{h}^{-1}$, Station 7 bin 1). Overall, variation between stations was not significantly different ($p = 0.48$, $n = 65$). No significant difference could be measured between bin 1 and bin 2, except for station 37 ($p = 0.048$).

Table 1: C fixation rates in different incubation bottles and Incubation bins. Shown are temperatures in incubation bins (InT) 1 and 2 as well as carbon fixation rates. Fixation rates in $\text{nmol C L}^{-1} \text{h}^{-1}$.

Station	SST (°C)	InT bin 1 (°C)	InT bin 2 (°C)	Rep. 1 bin 1	Rep. 2 bin 1	Rep. 3 bin 1	Rep. 1 bin 2	Rep. 2 bin 2	Rep. 3 bin 2
37	3.08	8.8	9.1	33.2	78.1	30	55.9	74.6	24.5
11	3.3	5.3	7.8	64.2	86	42.5	NA	NA	NA
E	4.7	12.9	12.7	111	92.2	129.8	108.3	112	108.2
7	5.59	12.5	12.9	39.3	67.9	58.2	179.4	120.2	67.4
9	5.84	8.4	8.6	148.1	134.9	NA	NA	NA	NA
6	6.3	10	11.1	51.2	64.1	28.2	176.8	93	81.1
14	11.59	18.3	18.6	69.6	160.3	137.6	41.4	115.2	134.9
15	15.44	21.8	22.2	65.8	97.6	72.2	NA	NA	NA
4	16.99	13.3	14.7	45.1	78.2	59.2	30.5	32.5	21.8
3	20.48	20.9	23.5	14.6	35.2	30.5	NA	NA	NA
16	23.78	NA	NA	15.4	22.4	14.2	7.1	22.4	13
2	25.78	24.2	27.1	7.1	11.5	13.5	7.8	5	2.6
18	27.38	NA	NA	14.5	15.5	14	11.9	10	9.4

Nitrogen fixation showed an inverse trend in comparison to absolute C fixation. High N₂ fixation rates ($2.3 \pm 2.2 \text{ nmol L}^{-1} \text{ d}^{-1}$; mean \pm SD, n = 24) were measured in the warm oligotrophic waters of the IO (stations 2, 3, 16, 18). Minima were measured in the productive zone of mixed water from IO and ACC (stations 4, 14, 15; $1.2 \pm 1.5 \text{ nmol L}^{-1} \text{ d}^{-1}$; mean \pm SD, n = 16). A slight increase ($2.0 \pm 0.8 \text{ nmol L}^{-1} \text{ d}^{-1}$; mean \pm SD, n = 6) in N₂ fixation could be measured in the PF/ Fawn Trough, station 37. In general, variation of N₂ fixation between different sea-surface temperatures (SSTs) was significant (p = 0.025, n = 65). However, variation between replicates was quite high as well, and could range between triplicates from 0.9 to 7.9 nmol L⁻¹ d⁻¹ (Station 18).

Ammonium assimilation was not significantly different between different SST (p = 0.74, n = 65). It ranged between 8.8 nmol L⁻¹ d⁻¹ (Station 2) and 105.1 nmol L⁻¹ d⁻¹ (Station E), with an outlier at station 15 ranging from 233.4 to 359.1 nmol L⁻¹ d⁻¹ between triplicates (Table 2). Nitrate assimilation was significantly different between different SSTs (p = 0.0007, n = 65). However, a clear relationship between N₂ fixation and SST could not be determined. In general, nitrate assimilation was very low ranging between 0.4 – 36.2 nmol L⁻¹ d⁻¹.

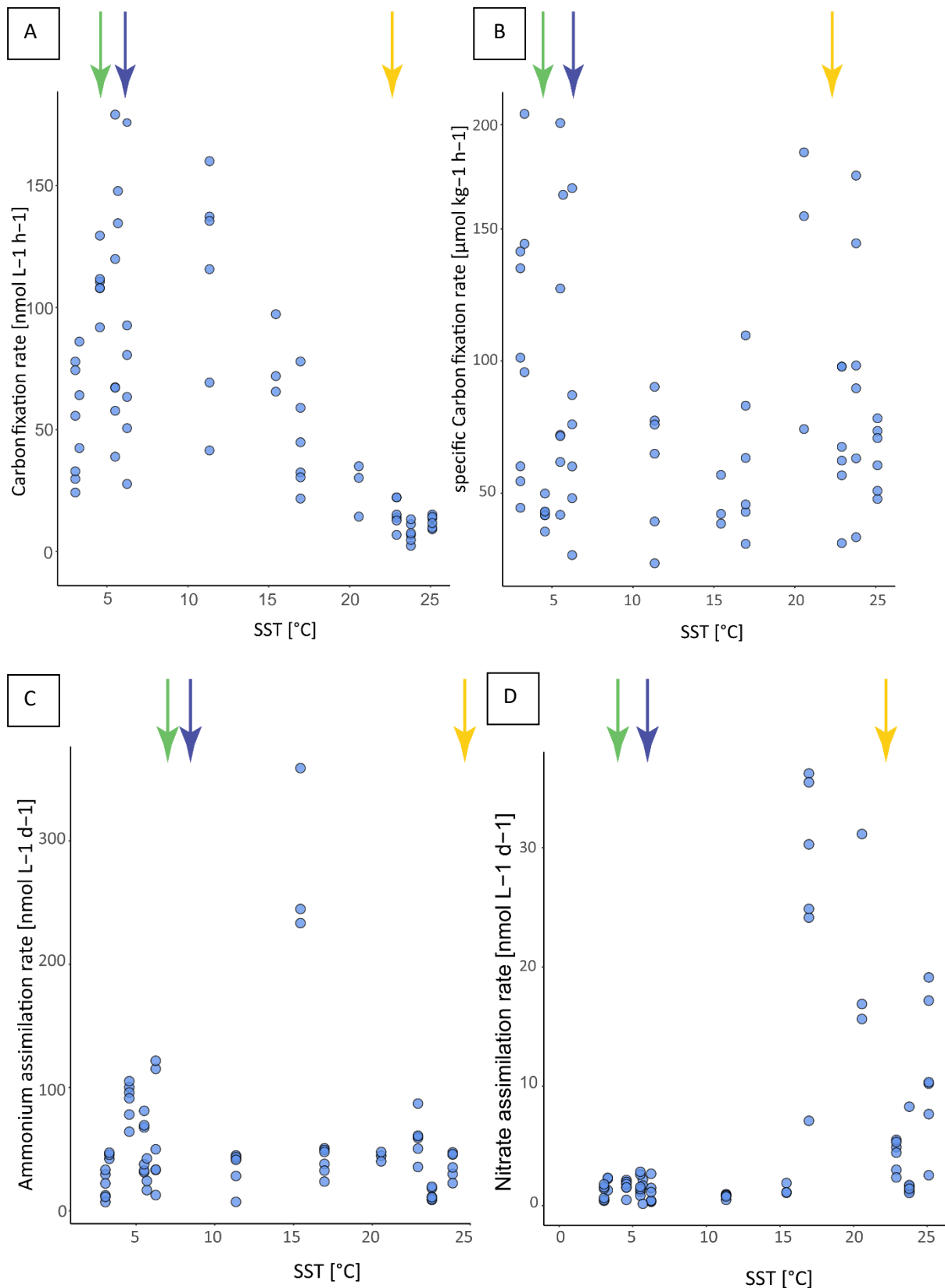


Figure 8: Carbon and nitrogen fixation rates against sea surface temperature (SST) from two different incubation bins with three replicates each. **A**, carbon fixation, followed a trend with relative high rates in the mixing zone between IO and ACC; trendline: $R^2=0.5$. **B**, chlorophyll a- normalized, specific carbon fixation rate against SST; **C**, Ammonium assimilation. **D**, Nitrate fixation rates having relatively higher rates in the warm water of the IO. Arrows indicate major fronts as described for figure 6.

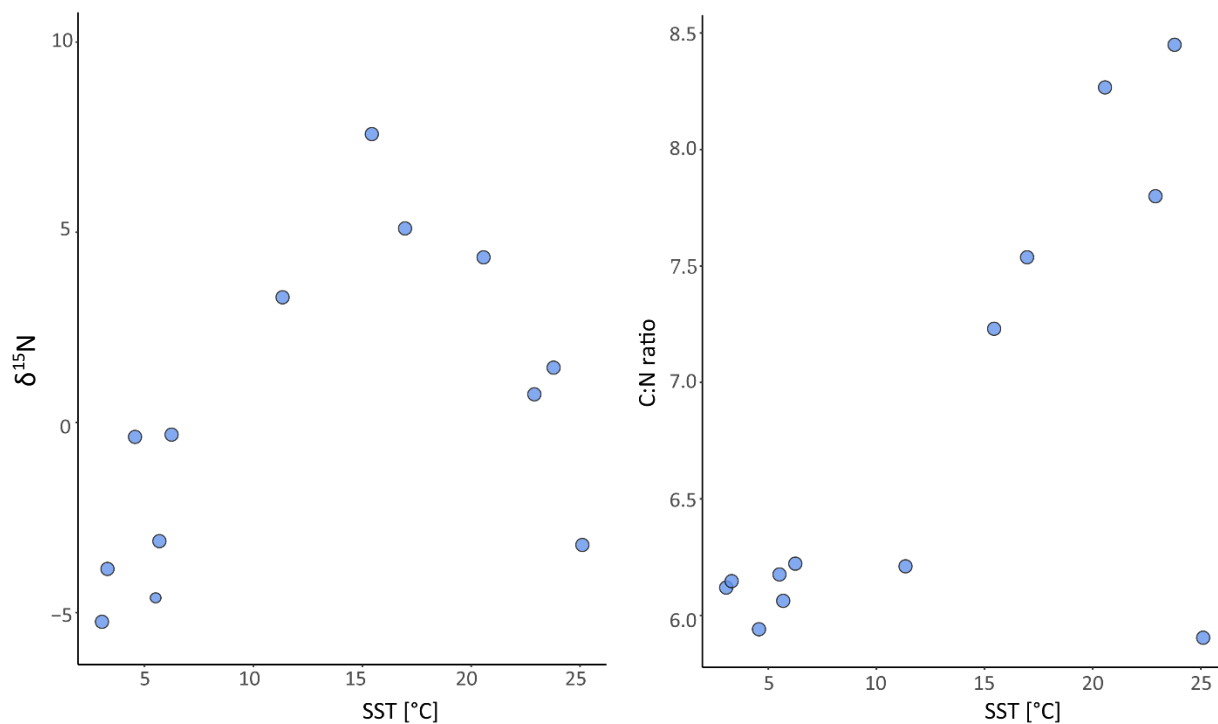


Figure 9: Relationships between particulate organic matter (POM) composition and sea-surface temperature (SST). **A**, Natural abundance of $\delta^{15}\text{N}$ from the particulate organic nitrogen (PON). Red lines are smoothing curves with a second polynomial order. **B**, POC: PON ratios in POM.

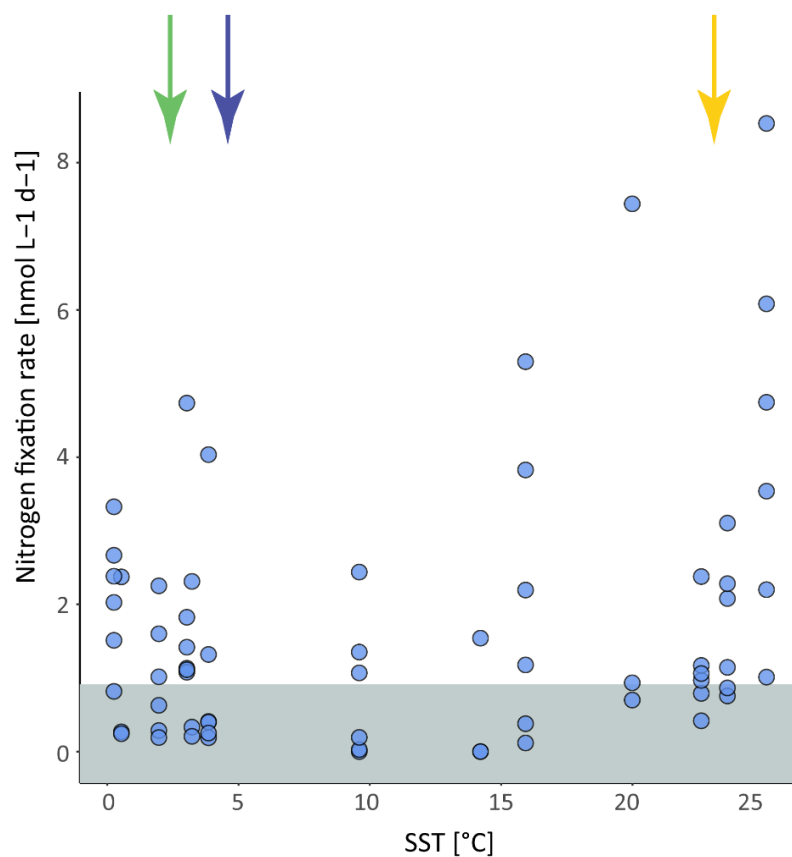


Figure 10: Nitrogen fixation rates shown in nmol N L⁻¹ d⁻¹. Grey bar indicates minimum quantifiable rate (MQR = 0.8 nmol N L⁻¹ d⁻¹).

Table 2: Sampling stations visited during the OISO cruise, including N₂ fixation, ammonium and nitrate assimilation rates. NA indicates no data. Standard deviation (average \pm STD; n = 3 for stations 3, 9, 11, 15; n = 6 for stations E, 37, 2, 4, 6, 7, 14, 16, 18).

Station	Longitude [°E]	Latitude [°S]	MLD [m]	N ₂ fix [nmol L ⁻¹ d ⁻¹]	ρ NH ₄ ⁺ [nmol L ⁻¹ d ⁻¹]	ρ NO ₃ ⁻ [nmol L ⁻¹ d ⁻¹]
E	72.367	48.79967	82.281	0.92 \pm 0.8	89.12 \pm 15.3	1.58 \pm 0.6
37	52.0025	55.00383	51.525	1.97 \pm 0.8	19.31 \pm 10.6	1.05 \pm 0.6
2	54.09983	30.0005	7.945	1.58 \pm 0.9	13.06 \pm 4.7	2.56 \pm 2.8
3	53.49933	34.99967	15.884	2.81 \pm 3.6	44.14 \pm 3.8	21.23 \pm 8.6
4	52.7895	40.0015	54.571	2.01 \pm 1.9	40.36 \pm 10.8	26.35 \pm 10.7
6	52.10233	45.00017	40.663	1.02 \pm 1.4	61.01 \pm 46.1	1.07 \pm 0.9
7	58.0035	47.66733	49.576	1.75 \pm 1.3	53.29 \pm 21.9	1.74 \pm 0.8
9	64.99917	48.5015	69.398	0.88 \pm 1.1	27.81 \pm 13.2	1.34 \pm 1.1
10	68.42117	50.66717	91.185	NA	NA	NA
11	63.00617	56.4985	47.556	0.89 \pm 1.1	44.92 \pm 2.5	1.96 \pm 0.6
14	74.884	42.49917	29.761	0.79 \pm 0.9	34.59 \pm 14.7	0.81 \pm 0.2
15	76.40683	39.99933	50.603	0.48 \pm 0.8	279.1 \pm 69.5	1.37 \pm 0.5
16	73.46633	35.0005	0	1.05 \pm 0.6	58.88 \pm 16.8	4.26 \pm 1.3
18	65.832	27.99983	23.835	4.04 \pm 2.5	37.72 \pm 10.3	11.18 \pm 6.1

Natural abundance of ¹⁵N in the PON fraction varied with SST, following a 2nd polynomial fit ($R^2 = 0.84$; n = 13). $\delta^{15}\text{N}$ ranged from -5.24 in the PF to 7.58 in the mixed water of the ACC and IO, where high productivity is also measured. $\delta^{15}\text{N}$ drops to -3.2 in the IO. The molar ratio between POC and PON is low in the PF and ACC (5.1-5.3) and increases in the mixed water of the ACC and IO until it reaches a maximum of 7.2 at 23.8°C (Station 2) in the IO. Unexpectedly, Station 18, having the highest SST in the IO, had the lowest ratio of just 5.0.

3.4 Community composition

3.4.1 Autotrophic pigment analysis based on High Performance Liquid Chromatography

Total biomass was relatively low, with an average pigment concentration of $0.176 \pm 0.05 \text{ mg m}^{-3}$ ($n = 7$) in warm water stations of the IO (Stations 2, 3, 16, 18; Fig 11 A) whereas all other stations had higher biomass (average $1.2 \pm 0.6 \text{ mg m}^{-3}$; $n = 16$). The pigment concentration of zeaxanthin was high in the IO (average $0.048 \pm 0.01 \text{ mg m}^{-3}$; Fig. 11 A) indicating a relative high abundance of prokaryotes (Fig. 11 B; Fig. 12 A). Zeaxanthin still occurred in mixed water of IO and ACC, but disappeared towards colder water of the ACC, PF and Fawn Trough. Besides prokaryotes in general, *Prochlorococcus* was highlighted through its diagnostic pigment divinyl

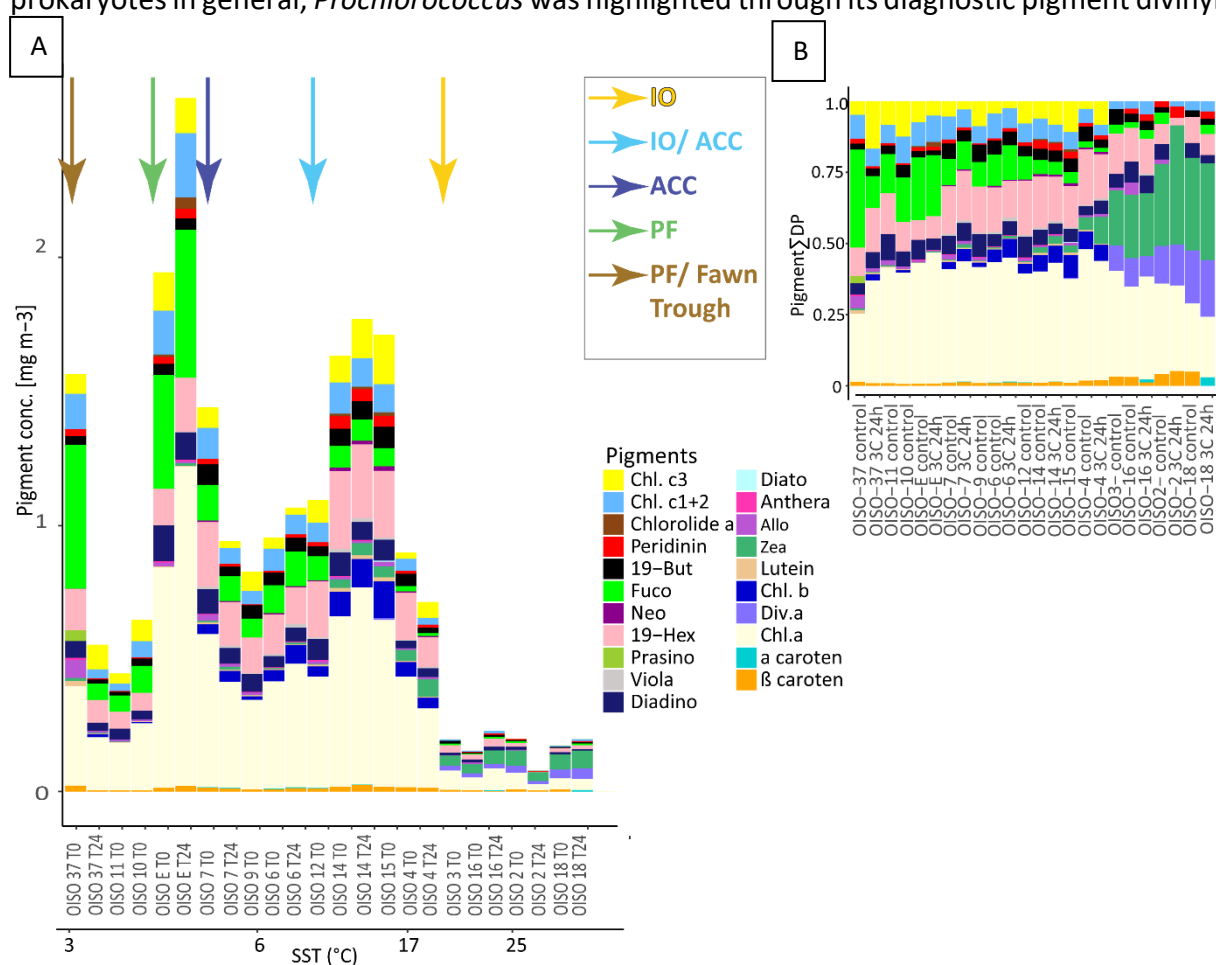


Figure 11: pigment analysis, showing (A) the relationship of different pigment concentrations for each station at T0 and T24. Stations are ordered according to their SST (non-linear). Arrows indicate changes of water masses. B, pigment concentrations normalized by total pigment concentration.

chlorophyll a (Fig. 11 B) and showed also a relative high abundance in the IO (Fig. 12 A). β -carotene had a relative high abundance in the IO as well (Fig. 11 B). Although dinoflagellates occurred in all water masses, they were slightly more relatively abundant in the IO.

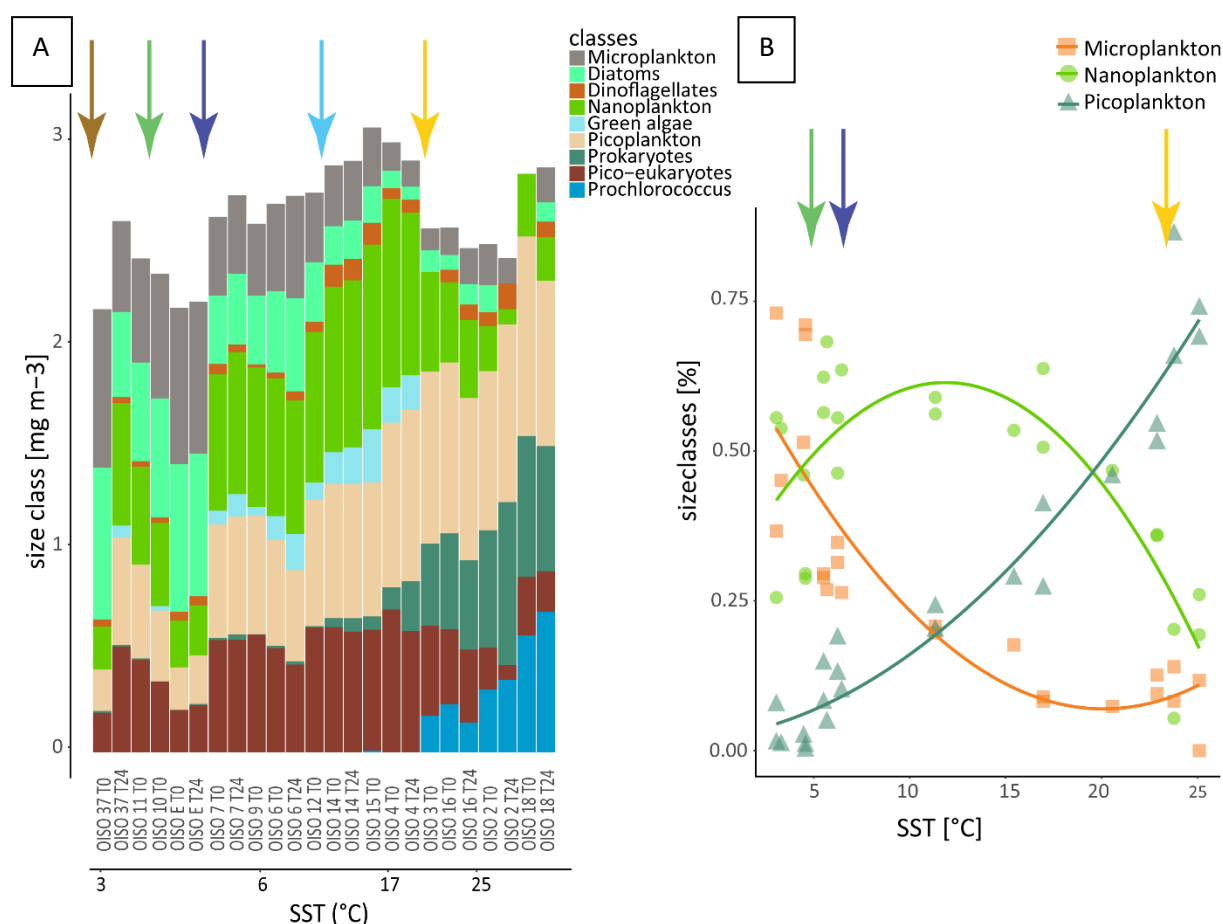


Figure 12: Phytoplankton functional types (PFTs) and Phytoplankton size classes (PSCs) against SST. **A**, relative abundance of different PFTs calculated after Hirata et al. (2011), stations are sorted after increasing temperature. **B**, relative abundance of size classes against SST calculated after Uitz et al. (2006). Brown arrow highlights the mixed water between PF and Fawn Trough, green arrow PF, dark blue arrow ACC, light blue arrow mixed water of ACC and IO and yellow arrow IO

Pigments such as chlorophyll c3 and peridinin (Dinoflagellates) appeared in mixed water from IO/ACC, ACC, PF and Fawn Trough (Fig. 11; Fig. 12 A).

Moreover, the concentration of 19'-hexanoyloxyfucoxanthin (19-Hex) was high in all stations in the mixed water from IO and ACC, ACC, PF and mixed water PF and Fawn Trough ($0.17 \pm 0.07 \text{ mg m}^{-3}$) in comparison to the IO ($0.017 \pm 0.009 \text{ mg m}^{-3}$; Fig. 11 A). 19-Hex is an accessory pigment found in the nano- to picoplankton size fraction such as pico-eukaryotes and prymnesiophytes (haptophytes).

Stations 14 and 15 (mixed water IO/ACC) as well as all stations in the ACC, PF and Fawn Trough had relatively high concentrations of fucoxanthin ($0.17 \pm 0.17 \text{ mg m}^{-3}$) which is an indicator for diatoms. Relative abundance of diatom concentration was highest in the PF and PF/ Fawn Trough (0.6 ± 0.1 , mean \pm SD, Fig. 12 A). Along with fucoxanthin, diadinoxanthin (Diadino) also appeared in those water samples and incubations. Diatoms were relatively more abundant in

the cold-water of the Fawn Trough and PF (Fig. 12 A) and continuously declined towards the IO. Green algae predominantly occurred in the ACC and mixed water of the ACC and IO, however, having a relative low abundance of the total phytoplankton community.

The phytoplankton size classes (PSCs; pico- nano- and microplankton) showed a clear pattern over SST variations (Fig. 12 B). While picoplankton dominated warm water in the IO, they sharply decreased ($R^2 = 0.94$, $p = 3.34 \times 10^{-13}$, $n = 24$) towards lower SST. Microplankton showed a contrary trend to picoplankton abundance, having high abundance in cold-water and decreasing towards warmer SST ($R^2 = 0.73$, $p = 1.27 \times 10^{-6}$, $n = 24$). However, they had a minimum at 20°C SST and slight increases towards 25°C SST. Nanoplankton had a maximum at 12°C SST and decreased both towards warmer and colder water ($R^2 = 0.61$, $p = 5.29 \times 10^{-5}$, $n = 24$).

Overall, the community composition as well as the total biomass did not change significantly between T_0 and T_{24} (Fig 11, Fig. 12 A).

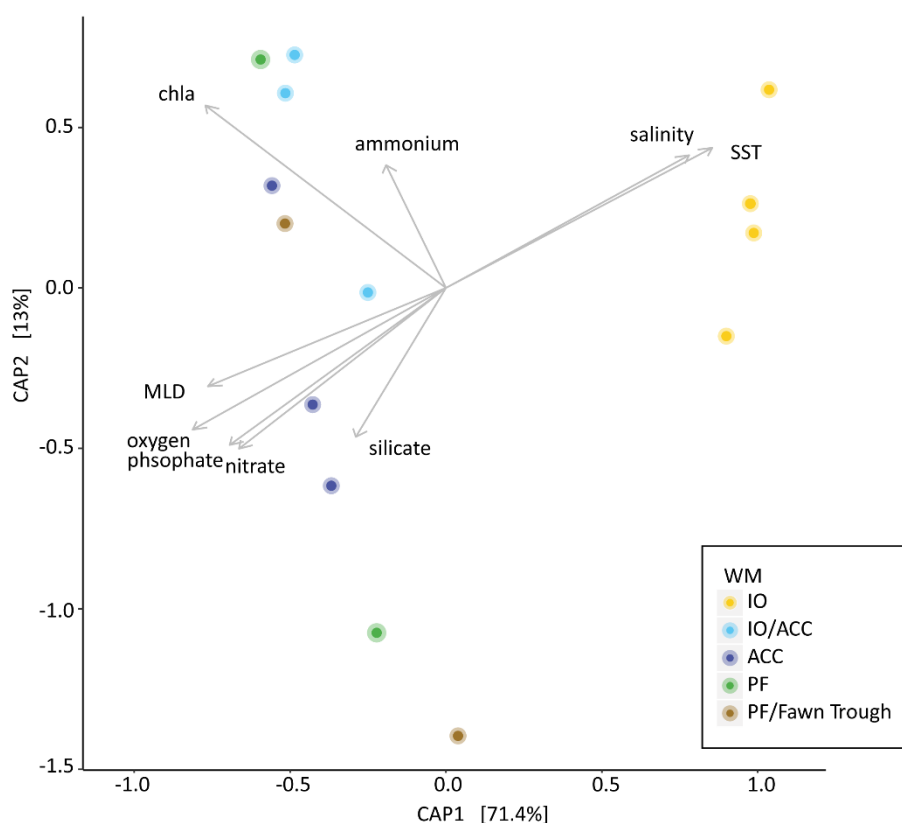


Figure 13: Microbial photoautotrophic community structure of different water masses. Constrained Analysis of Principal Coordinates (CAP) of pigment concentrations (HPLC). Pigment concentrations were used to calculate Bray- Curtis distances and constrained analysis was performed by water mass. Constrain reflects 84.4 % of overall variance in the data. There was a significant relationship between water masses and community dissimilarity (adonis test; $p < 0.001$). Different water masses were coloured according to the legend; water mass (WM); Indian Ocean (IO); mixed water of Indian Ocean

and Antarctic Circumpolar Current (IO/ACC); Antarctic Circumpolar Current (ACC); Polar Front (PF) and mixed water of Polar Front and Fawn Trough (PF/Fawn Trough). Data with environmental samples represented as arrows.

Constrained analysis of the HPLC data revealed significant differences between the water masses (adonis test; $p < 0.001$) (Fig. 13). However, only samples of the IO clustered together. Additionally, both salinity and SST were associated with the IO samples. Samples of all other water masses could not be separated according to their similarity. Samples of the cold-water stations were more associated with nutrient concentrations, oxygen concentration, chlorophyll *a* concentration and MLD.

3.4.2 16S rDNA amplicon sequence analysis

16S Amplicons: From each of 14 stations small subunit ribosomal protein DNA (16S) was amplified and sequenced to obtain insights into the diversity and community composition of both bacteria and archaea. To monitor potential shifts in community composition in the incubation bins we took samples from 9 x 24h incubation bottles. 5600 OTUs were recovered using local threshold clustering technique which represents biological needs better than arbitrary cut-offs. Sequence reads of 16S amplicon data showed no conspicuous outliers (appendix S-5).

OTU richness was significant (linear fit) higher in the IO and in the mixed water of the IO and ACC in comparison to the cold-water stations (Fig.14). Alpha diversity was highest at station 15 in the mixed water of the IO and ACC. Both Richness and alpha diversity normally did not change significantly between the T_0 sampling event and 24h incubation. There was no clear preference for higher richness or diversity between T_0 and T_{24} . However, the 24h incubation at station E showed a significant increase in both richness and diversity in comparison to the T_0 sample.

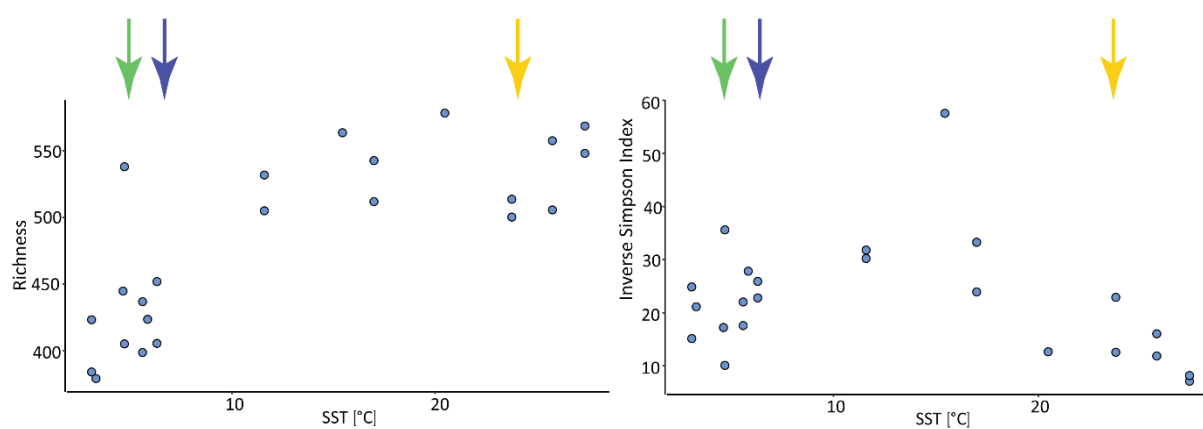


Figure 14: **A**, OTU richness of 16S amplicon sequences changing over SST. **B**, Alpha diversity of OTUs calculated as inverse Simpson Index against SST. Arrows indicate major fronts as described in figure 6.

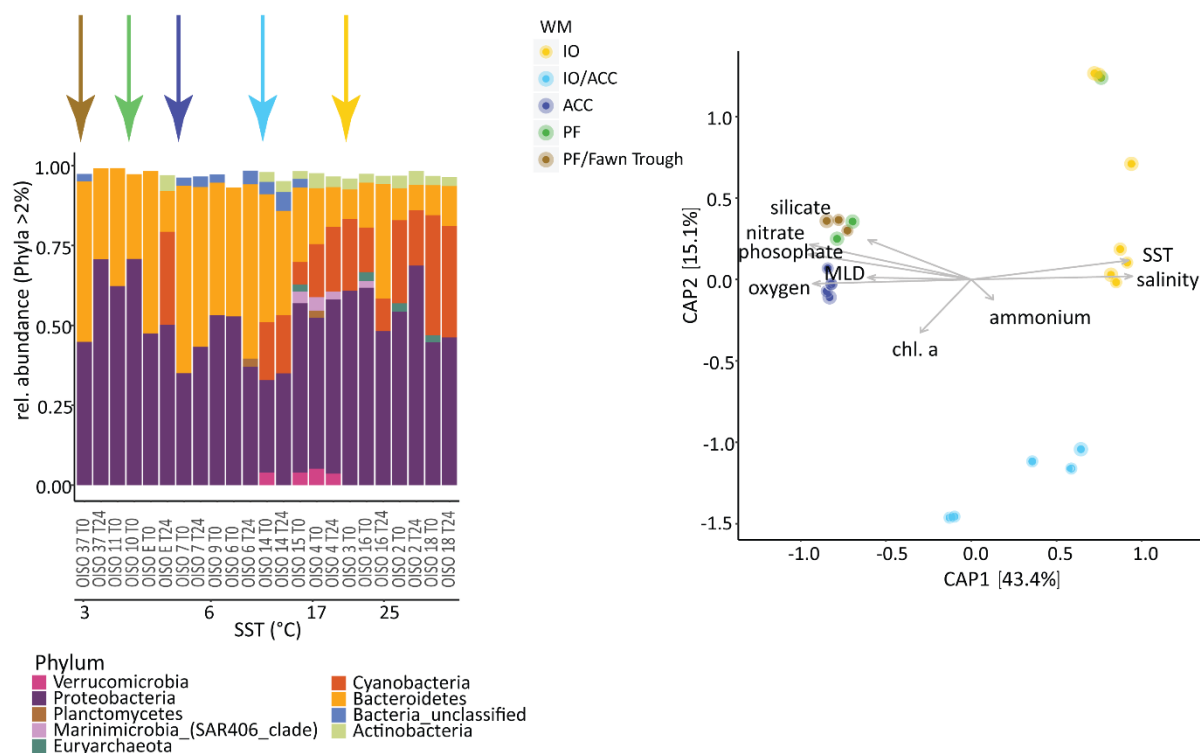


Figure 15: A, relative abundance of phyla for each station and within incubations. Arrows indicate major water masses according to the legend; Indian ocean (IO), mixed water of Indian Ocean and Antarctic Circumpolar Current (IO/ACC), Antarctic Circumpolar Current (ACC), Polar Front (PF), and mixed water of Polar Front and Fawn Trough (PF/Fawn Trough). **B**, Bacterial community structure of different water masses. Constrained Analysis of Principal Coordinates (CAP) of 16S rDNA diversity. OUT abundance table was used to calculate Bray- Curtis distances and constrained analysis was performed by water mass. Constrain reflects 58.5 % of overall variance in the data. There was a significant relationship between water masses and community dissimilarity (adonis test; $p < 0.001$). Data with environmental samples represented as arrows.

Within the phylum level, all stations were dominated by Proteobacteria. Alphaproteobacteria were the most dominant order within the proteobacteria. Second most abundant were bacteria belonging to the phylum Bacteroidetes, however, their relative abundance decreased towards warmer SST in the IO. Instead, Cyanobacteria occurred in the mixed water of the IO and ACC and in the IO. By looking at a higher resolution at the phylogeny (Fig.16) one can see that the IO is mostly dominated by *Prochlorococcus sp.* with relatively low abundance of *Synechococcus*, except Station 4 where we found 100% *Synechococcus* within the Cyanobacterial fraction. In addition, Actinobacteria occurred in relative constant fraction throughout all IO/ACC and IO water samples. We found ~5% OTU abundance annotated to the phylum Verrucomicrobia in the IO/ACC waters. Prokaryotes belonging to the kingdom Archaea were found in abundance over 2% only in 4 samples all belonging to the phylum Euryarchaeota. The ACC and PF show a high relative abundance of the order Flavobacteriales

within the phylum Bacteroidetes. Moreover, we found a great dominance of ecotype Ia, Ib and II of SAR11 clade throughout all samples. Notably, the 24h incubation which already showed high diversity and richness, showed a similar pattern to the IO samples in the relative abundance of prokaryotic phyla. This pattern is also represented in the CAP analysis where all stations separate according to the water masses they are in, except the 24h incubation of Station E. Stations of the ACC, PF and mixed water of PF and Fawn Trough were all relatively similar to each other, while stations in the IO and mixed water of the IO and ACC showed greater variability, similar to the results from the richness calculations. We assume, these results were due to wrong labelling or processing of the sample and will not be taken further into account in the analysis.

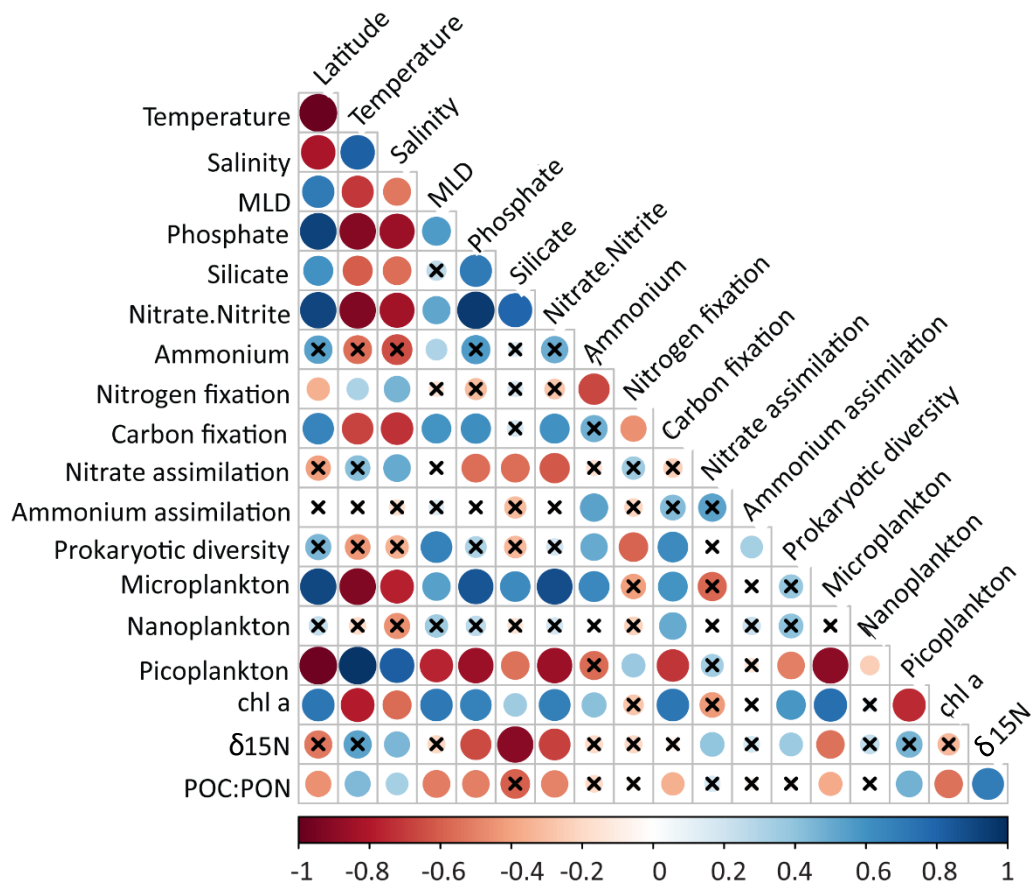


Figure 17: Spearman correlation coefficients (r_s) plot including NO_3^- and NH_4^+ assimilation, C fixation and N_2 fixation rates as well as PSCs ($n=13$). For prokaryotic diversity, PSCs and chl a only T_0 samples were used for correlation calculations. Blue colour indicates positive correlation, red negative correlation. Cross indicates no significant correlation (significance level: $p = 0.05$).

Several significant correlations occurred between physical-chemical parameters (temperature, salinity, nutrient concentration, respectively) and C fixation, N assimilation and phytoplankton size classes (PSCs; Fig. 17).

Noteworthy was a positive correlation between N_2 fixation and salinity ($r_s = 0.47$). N_2 fixation rates did not show any significant correlations with either NH_4^+ or NO_3^- assimilation rates. N_2 fixation revealed a significant negative relationship with C fixation ($r_s = -0.46$). Furthermore, N_2 fixation was positive with the picoplankton component ($r_s = 0.55$). In contrast, N_2 fixation was negative associated with prokaryotic diversity ($r_s = -0.59$).

C fixation was negatively correlated with temperature and salinity ($r_s = 0.68$, $r_s = 0.72$, respectively). In addition, C fixation was positive correlated with NO_x concentration. Both

microplankton and nanoplankton were positively correlated with C fixation, while picoplankton concentrations were negatively correlated.

NO_3^- assimilation rates did not show many significant relationships with other rates or environmental parameters other than a significant negative correlation with PO_4^- , NO_x and Si concentration and positive relationship with salinity. NH_4^+ assimilation was positively correlated with NH_4^+ concentration ($r_s = 0.77$).

Microplankton abundance correlated negatively with temperature and salinity, but positively with all nutrients ($r_s = 0.79, 0.52, 0.79$ and 0.58 for PO_4^- , Si, NO_x and NH_4^+ , respectively; Fig. 17). Prokaryotic diversity was positively associated with MLD, C fixation and ammonium concentration. $\delta^{15}\text{N}$ had a positive relationship with prokaryotic diversity ($r_s = 0.37$) and POC: PON ratio ($r_s = 0.69$) but was negatively associated with all nutrients.

4. Discussion

The OISO (Ocean Indien Service d'Observation) campaign aims to understand the seasonal and temporal fluctuations of the Indian Ocean (IO) and the Southern Ocean (Indian Ocean sector) carbon budget. The program's longterm goals are for a better knowledge about carbon budget evolution and ocean acidification, as well as improving the global prognostic climate models such as the Global Carbon Project and the Global Ocean Acidification Observation Network (IPCC, 2014). The global carbon cycle is tightly connected to the nitrogen (N) cycle in oceanic ecosystems (reviewed in Gruber and Galloway (2008)). N is a key element for all kinds of biological processes, such as protein synthesis and cellular growth (reviewed in Gruber, 2008). Thus, the input of N into aquatic ecosystems potentially stimulates additional C fixation (e.g. Boynton et al., 1982). N is an essential building block for all organisms, where it generally accumulates at the POC: PON ratio in marine organic matter described as the Redfield ratio (6.625; Redfield, (1958)). However, several factors can cause a deviation from this ratio, including nitrogen- and light-limitation, zooplankton abundance (Talmy *et al.*, 2016) and the activity of heterotrophic microbes (Crawford *et al.*, 2015). A fundamental process influencing the balance between C and N is the fixation of atmospheric N₂ by diazotrophs, which provide organic N for both phytoplankton growth and C fixation. Our data, as part of the OISO campaign, contribute to a better understanding of the physical and biological factors controlling C and N cycling processes in four different water masses of the Southern Indian Ocean and regional waters of the French Southern and Antarctic islands, during Austral summer January and February 2017.

The physical (T, S and O₂) and biochemical parameters (DIN, DIC, PO₄⁻ and Si) allowed us to distinguish clear differences between water masses of the Indian Ocean (IO), Antarctic Circumpolar Current (ACC), Polar Front (PF) and Fawn Trough in surface waters. However, there was a distinct boundary between the IO and the ACC about 1000 m below the surface. The mixed layer depth (MLD) was deepest above the Kerguelen plateau, which is consistent with the measurements of Blain et al. (2007) and Mongin et al. (2008) for the summer season. A deep MLD can be caused by high internal tidal waves (Park *et al.*, 2008 (a)). This process is also the reason inferred for elevated Iron (Fe) concentrations above the plateau, which leads to extensive phytoplankton blooms (Blain *et al.*, 2007).

Major differences in water mass chemistry were observed (high SST and salinity in the IO) which were associated with lower dissolved gasses and nutrients, possibly because cold water can hold more dissolved oxygen and DIC. DIC concentrations in seawater are a function of temperature, but also a function of salinity and partial pressure of CO₂ (Henry's law). There was a clear increase of DIC concentration between 1998 and 2017 throughout the whole sampling area, likely due to an anthropogenic increase of atmospheric pCO₂ in the past years (>400ppm; Tans and Keeling, 2018).

The long-term data did not show significant differences in nutrient concentrations over the past 9 years, suggesting a relatively stable nutrient pool in these waters. The Fawn Trough, PF and ACC contained higher nutrient concentrations, likely due to upwelling in the Southern Ocean. Although nutrient concentrations are relatively high, primary productivity remains low due to iron limitation (Blain *et al.*, 2007). This phenomenon is described as a high nutrient low chlorophyll situation (HNLC; Blain *et al.*, 2007; Hart, 1942; Sullivan *et al.*, 1993; Tyrrell *et al.*, 2005). N* is negative in cold-water, potentially indicating N limitation or P excess. This is congruent with the findings by Weber and Deutsch (2010) with N* ~ -2 in the PF zone. This can be interconnected with high diatom abundance which have a N:P ratio of 11:1 rather than the normal 16:1 (Weber and Deutsch, 2010). In contrast, González *et al.* (2014) measured a positive N* in the adjacent naturally iron-fertilized waters above the Kerguelen plateau. A positive N* originates through deposition of N-rich material from the atmosphere, N₂ fixation and/or export of P-rich material (Blain *et al.*, 2015). In this case, we infer that an indirect influence of dFe on an oversaturated N pool, for instance through supporting N₂ fixation, is most likely (González *et al.*, 2014).

The POC: PON ratio across all the water masses within our study was almost exactly the Redfield Ratio (6.7±0.9). However, we showed POC: PON ratio has a linear relationship with SST across the range from 5.9 to 8.4. These findings match the observation by Martiny *et al.*, (2013) of higher (>7) POC: PON ratios in high-temperature, low nutrient waters than in low-temperature and high nutrient waters (~6). Increasing chlorophyll biomass is negatively correlated with POC:PON ratios (Martiny *et al.*, 2013), which we also observed. Low POC: PON ratios can occur for instance through high abundance of heterotrophic microbes and lower abundance of larger cells, such as diatoms and dinoflagellates (Crawford *et al.*, 2015). Furthermore, different life strategies, such as growth rate (r/K- selection), the ability of algae

to store nutrients in internal pools (Arrigo, 2005) or selfish substrate uptake in prokaryotes (Reintjes *et al.*, 2017) can potentially further influence the cellular C:N ratio. The impact of these processes in our study, however, remain still unknown and needs to be elucidated in future. Our data show a reversed trend to the findings proposed by Crawford *et al.* (2015), having increased abundance of larger cells and the PFT diatoms along with decreased POC:PON values. The proportion of chl *a* to total POC decreases from low SST to high SST, likely indicating that the proportion of heterotrophic organisms increase towards higher SST (Appendix S-4). This could be a reason for the shifted POC: PON ratios, having lots of nitrate saturated autotrophs in the PF and ACC, and more heterotrophic organisms in the IO which potentially need less N than autotrophs (Martiny *et al.*, 2013).

In the face of human induced climate change and resulting increased stratification of the ocean (Capotondi *et al.*, 2012), nutrient supply [from below] could alter the community composition (Arrigo, 2005). For instance, in the polar regions, a shift towards higher diatom abundance is possible (Arrigo, 1999, 2005). Diatoms prefer stratified waters and have low N:P requirements. As a result, global nutrient inventories could be influenced by such a change in community composition, such as the depletion of NO_3^- relative to PO_4^- (Arrigo, 2005).

Supplies of inorganic N and organic N are controlled via different processes including vertical and lateral transport (Torres-Valdes *et al.*, 2009), grazing, excretion and viral lysis (Azam *et al.*, 1983). Assimilation rates of both NO_3^- and NH_4^+ provide insights into production and turnover at the base of the food web. Which process dominate the N pool is reflected in the particulate organic matter (POM) elemental composition. Organisms prefer to take up light isotopes of macronutrients, because of their faster reaction rates in comparison to heavy isotopes. Therefore, $\delta^{15}\text{N}$ can drop below seawater standard in nutrient saturated environments or where N_2 fixation is the primary source for new N (Carpenter *et al.*, 1999; Montoya, Carpenter and Capone, 2002; Montoya, 2007). These processes were evident in our dataset, having nitrate excess in the HNLC areas of the PF and ACC with accompanying $\delta^{15}\text{N}$ values below the standard and negative $\delta^{15}\text{N}$ in the IO where N_2 fixation has a relative high contribution to primary productivity. In the mixed water of the ACC and IO, $\delta^{15}\text{N}$ was relatively high suggesting a consumption of subsurface nitrate (Fawcett *et al.*, 2014) as well as the transfer of N to higher trophic levels (Montoya, 2007). These findings also match our nutrient measurements, which showed low macronutrient concentrations $>15^\circ\text{C}$ SST. In the following section we discuss the

different N- cycling processes in conjunction with primary productivity and microbial community composition.

Prokaryotic community composition

Overall, bacterial community was dominated by Proteobacteria, Cyanobacteria and Bacteroidetes. All samples showed a large fraction of the ubiquitous alphaproteobacterial SAR11 clade. SAR11 reach their largest numbers in stratified, oligotrophic gyres, mainly harvesting low-molecular-weight DOM (Giovannoni, 2017). The SAR11 clade is grouped into several subclades each of which is associated with specific environmental and seasonal parameters (Giovannoni, 2017). We found ecotypes of Cluster Ia, Ib and II throughout our samples; all are described as surface ocean associated clades, while cluster Ib and II specifically occur in spring and summer season.

The IO was characterized by high abundances of cyanobacteria and some actinobacteria. Cyanobacterial fraction was dominated by *Prochlorococcus* and *Synechococcus*. These organisms are considered the most abundant photosynthetic organisms in the ocean (Waterbury *et al.*, 1986; Partensky, 1999(a); Hess and Vaultot, 1999). In co-occurrence, *Prochlorococcus* is the dominating species (Partensky, 1999(a); Blanchot and Vaultot, 1999). Our data supports this observation with little relative abundance of *Synechococcus* (1-5%) in conjunction with *Prochlorococcus* (95-99%). The mixed water of the IO and ACC is more diverse, and contains, among others, some bacteria belonging to the phylum Verrucomicrobia which has been described to be characteristic for south of the PF south of Australia in austral summer (Wilkins *et al.*, 2013). Bacterial communities in the ACC and PF were overwhelmingly dominated by Bacteroidetes, especially of the order Flavobacteria. Flavobacterial abundance has been observed to be tightly coupled with diatom concentration (Pinhassi *et al.*, 2004) since these bacteria specialize on successive decomposition of algal- derived organic matter (OM) (Teeling *et al.*, 2012). Flavobacteria have also been associated with marine snow due to their ability to break down highly complex OM (Edwards *et al.*, 2010; Thomas *et al.*, 2011; Gómez-Pereira *et al.*, 2012).

The microbial composition was distinctly more similar within the same water mass than between water masses. The greatest differences could be measured between the cold-water stations of the ACC and PF and the IO. We found a high influence of nutrients on microbial diversity within the PF and ACC, with temperature and SST more clearly influencing the IO

samples. Notably, having a high temperature influence in the IO waters, we measured relative high concentration of β carotene, which is known as a photoprotective pigment (Paerl, 1984). Remarkably, the mixed water of the IO and ACC did not show any association with other water masses. We conclude that the mixing process causes unique environmental sorting of bacterial populations. This data is in agreement with Baltar & Arístegui (2017) who highlighted the importance of permanent fronts as oceanographic features which may account for microbial community composition and activity. Furthermore, we found highest OUT diversity within this mixed water of the IO and ACC suggesting high niche partitioning. OUT richness was also highest in the mixed water of the IO and IO/ACC. However, diversity was relatively low in the IO suggesting low evenness of bacterial OTUs. Since we found a great proportion of *Prochlorococcus* (or *Synechococcus*) in the IO, we conclude that evenness is greatly influenced by the vast dominance of *Prochlorococcus* (or *Synechococcus*) along with very diverse other species with low abundance.

Carbon fixation

Carbon fixation was highest above the Kerguelen plateau, potentially stimulated by high Fe concentrations (Blain *et al.*, 2007). However, it needs to be noted that Fe availability is not the only limiting factor in the Southern Ocean. Light and/or silicate can both play important roles in phytoplankton growth and in the accumulation of biomass (Boyd *et al.*, 2000). In general, we noted high C fixation values in the IO/ACC and ACC and lower C fixation both in colder and warmer SSTs. Notably, when C fixation values were normalized to chl *a* concentrations, no significant difference could be measured between sites suggesting that specific productivity did not vary greatly.

Differences in phytoplankton biomass and, associated therewith, lower absolute C fixation rates, can be interpreted as evidence for top down control instead of bottom up control. Cavagna *et al.* (2015) describes an increase of primary productivity per unit biomass associated with an increase in total biomass in the adjacent Kerguelen region waters in spring. This relationship collapses in summer and, typical for a post-bloom situation, the community composition shifts from autotrophic to predominantly heterotrophic organization suggesting a top-down control of phytoplankton biomass (Christaki *et al.*, 2014; Cavagna *et al.*, 2015). Our study region crossed the edge of the Kerguelen region with its massive naturally iron-fertilized spring blooms, and we infer that community composition at the sites we visited

could still have been influenced by such events. Our data show lower chl a : total POC ratios in the IO than in the (non-nutrient limited) PF (Appendix S-4), demonstrating that the IO is likely to be dominated by heterotrophic organisms. Carbon fixation rates in the IO showed little variation between replicates, while differences between replicates were relatively high in the other water masses. González et al. (2014) reported similar patterns for their N₂ fixation rate measurements. Great variations between replicates can be the result of a strong heterogeneity in the sub-mesoscale dynamics of water masses, especially in the PF, ACC and mixed water of PF and Fawn Trough and IO and ACC. These complex conditions also have been observed by Mongin et al. (2008) highlighting the importance of high resolution studies and the development of new and specific tools to assess reasons shaping such heterogeneity.

We could not find a relationship between prokaryotic diversity and absolute C fixation rates. We infer that the community composition *per se* has no significant impact on C fixation. However, certain prokaryotic groups can certainly contribute significantly to C fixation. We found that in the IO, prokaryotes make up a large fraction of total autotrophic organisms. *Prochlorococcus* is the most abundant photosynthetic organism on earth (Partensky, 1999(b); Hess and Vaulot, 1999). However, it does not occur in cold, high- latitudinal waters (>40°S/N). Our data confirms this hypothesis; analysis of 16S rDNA, as well as pigment analysis, revealed that *Prochlorococcus* of the phylum Cyanobacteria had a relative high abundance in the IO but were not found in the ACC and PF. Phytoplankton within the PF are typically dominated by larger diatoms (Lutjeharms, Walters and Allanson, 1985; Laubscher, Perissinotto and McQuaid, 1993; Dafner and Mordasova, 1994; de Baar *et al.*, 1995; Jochem, Mathot and Quéguiner, 1995; Smetacek *et al.*, 1997; Brown and Landry, 2001; Moore and Abbott, 2002). In addition to trace element deficiency and unfavourable light conditions, strong grazing pressure is considered a significant limiting factor for primary production in the Southern Ocean (Hart, 1942; Smetacek, Assmy and Henjes, 2004). Bigger cell sizes and hard frustules can be of advantage as protection against predators (Price, Ahner and Morel, 1994; Sherr and Sherr, 1994; Selph *et al.*, 2001). The relative abundance of nano- and microplankton size classes increased within the ACC and PF, while picoplankton decreased to undetectable concentrations. Additionally, we could show that the relative abundance of diatom species was high in the ACC and PF (up to 74%).

Interestingly, in the mixed waters of the IO and ACC, where we measured relatively high C fixation rates, both autotrophic biomass and prokaryotic diversity was exceptionally high. Furthermore, pigment analysis revealed a great diversity of all kinds of different pigments in this region. Additionally, the prokaryotic fraction is remarkably diverse (Inverse Simpson Index = 57.6). These observations are in accordance with one out of two major ecological mechanisms driving marine biodiversity: (1) diversity increases with increasing productivity, i.e. more resources can drive niche partitioning and (2) diversity increases with increasing temperature due to kinetic metabolism (Fuhrman *et al.*, 2008). A strong positive correlation between primary productivity and bacterial diversity has been observed in the PF zone (Wilkins *et al.*, 2013). Additionally it has been postulated that primary productivity plays a major role in determining bacterial richness, while temperature gradients are of less importance (Raes *et al.*, 2017). We note, that our data revealed a great difference between 16S richness and 16S diversity. For instance, we observed a positive correlation ($r_s = 0.5$) between primary productivity and diversity but a negative correlation ($r_s = -0.5$) between primary productivity and richness. Bacterial richness was highest in the IO and in the mixed water of the IO and ACC. We observed a predominance of the Cyanobacterium *Prochlorococcus* in these waters which gives rise to the assumption that OTU richness is high in these waters, thus evenness is low due to the vast dominance of *Prochlorococcus*. Absolute primary production and autotrophic biomass was relatively low in the IO and to a great extent driven by *Prochlorococcus*. In the mixed water of the IO and ACC and the in the ACC proper, diatoms, green algae, prymnesiophytes and pico- eukaryotes (all pos. correlated with C fixation) were the dominant primary producers. Moreover, we could measure pigment concentration on a large variety of all kinds of different pigments, indicating a great diversity in the photoautotrophic fraction. We speculate that not only primary productivity itself but also diversity and community composition of primary producers have a great impact on the prokaryotic diversity.

The $\delta^{15}\text{N}$ reaches its maximum value (7.58) at the same high-diversity station, supporting the notion of a very complex and diverse (microbial) community composition on many trophic levels. This, in turn, can support further the idea of niche partitioning (Menge and Sutherland, 1976; Huston, 1979; Polis and Strong, 1996). Canonical analysis of 16S OTUs did not strongly associate with a specific environmental parameter (minimal positive correlation with

ammonium concentration and chl *a*), however, it cannot be excluded that the supply of trace elements, such as Fe, could control diversity and productivity in this region.

N₂ fixation

N₂ fixation is a process with high energy costs, because of the strong triple bond in the N₂ molecule. Therefore, it has been assumed that N₂ fixation occurs predominantly in oceanic regions with limited organic N availability such as the subtropical gyres (Mather *et al.*, 2008). The chain forming cyanobacterium *Trichodesmium* dominates these warm, oligotrophic waters and has been postulated to contribute significantly to the global N budget (estimated to about $1.6 \cdot 10^{-1}$ in the tropical North Atlantik; Capone *et al.*, (2005)). However, a great diversity of bacterial *nifH* have been obtained also outside the (sub-)tropical region (Moisander *et al.*, 2010; Bentzon-Tilia *et al.*, 2015; Messer *et al.*, 2015; Scavotto *et al.*, 2015; Fernández-Méndez *et al.*, 2016; Martínez-Pérez *et al.*, 2016) suggesting an underestimation of both N₂ fixation rates and the diversity of diazotrophs.

Raes *et al.* (2015) showed that N₂ fixation rates in the eastern Indian Ocean were independent of the availability of other sources of DIN. Trace micronutrient availability, such as iron, can also limit growth and activity of diazotrophic organisms (Raven, 1988; Falkowski, 1997). Our data show higher rates in the oligotrophic water of the IO, however, measurable nitrogen fixation rates occurred throughout the whole sampling area. Noteworthy is a slight increase in N₂ fixation in the PF/Fawn Trough. Replicates showed a great rate heterogeneity, which was also described by González *et al.* (2014) above the adjacent Kerguelen plateau. This could imply submesoscale physical and potential biological parameters influencing the N₂ fixation efficiency. Interestingly, we found a stronger correlation of N₂ fixation with salinity rather than temperature, rejecting the hypothesis that temperature acts as the main driving factor for N₂ fixation rates. Overall, N₂ fixation rates were comparable to N₂ fixation rates measured by González *et al.* (2014) above the Kerguelen plateau. We found a strong positive correlation between N₂ fixation and *Prochlorococcus* ($r_s = 0.68$) abundance. However, *Prochlorococcus* is not capable of N₂ fixation, but generally prefers warm SSTs (Johnson *et al.*, 2006) just as the highly abundant diazotroph *Trichodesmium* (Capone, 1997; Karl *et al.*, 2002; Hood, Coles and Capone, 2004; Breitbarth *et al.*, 2007).

Every species has its temperature optimum. It is known that diazotroph activity is very sensitive to both physical (e.g., temperature) and chemical changes (Barcelos e Ramos *et al.*,

2007; Breitbarth *et al.*, 2007; Hutchins *et al.*, 2007; Levitan *et al.*, 2007; Rost, Zondervan and Wolf-Gladrow, 2008). We note that temperature in incubation experiments could not be kept stable because of logistic limitations, and ranged between maximum values of -7.7°C below and 9°C above the in-situ temperatures of the water samples. Both underestimation and overestimation of the N_2 fixation rates are therefore possible. We therefore consider relative measurements rather than absolute values in our analysis. Our data highlights the importance of a careful setup of perturbation experiments, with a strong necessity to keep continuous track of temperature.

Overall, our data contribute to closing the gaps in global N_2 fixation rates, especially considering previous underestimation of N_2 fixation at higher latitudes. We could show that N_2 fixation occurs independent of nitrate concentration rejecting the hypothesis from Breitbarth *et al.* (2007) that N_2 fixation just occurs when other sources of N are limited. We note, however, that N_2 fixation and ammonium concentrations are negatively correlated.

NO_3^- assimilation

In contrast to ammonium assimilation, nitrate assimilation is a more energy-intensive process because NO_3^- must be reduced to NH_4^+ prior to metabolic usage (McCarthy, 1981; Syrett, 1981; Berges and Mulholland, 2008). Still, measured NO_3^- uptake rates can exceed NH_4^+ assimilation (Cavagna *et al.*, 2015). The turnover of N has been suggested to be relatively rapid in the south-eastern Indian ocean (Beaufort, 1997; Thompson *et al.*, 2011; Waite *et al.*, 2013), having a significant impact on the biogeochemical nutrient cycling (Codispoti *et al.*, 2001; Hoegh-Guldberg and Bruno, 2010). Regeneration of NO_3^- can also occur rather close to the surface, so the concentration of NO_3^- varies at a weekly timescale. In our data, high NO_3^- assimilation rates were measured where the nutrient rich water of the ACC mixed with the warm oligotrophic IO. These stations contained high biomass (~ 1.7) and high C fixation rates ($\sim 94 \text{ nmol L}^{-1} \text{ h}^{-1}$). The $\delta^{15}\text{N}$ of the POM was also exceptionally high, suggesting transfer of POM to higher trophic levels. NO_3^- assimilation rates showed a strong negative correlation with nutrient availability indicating a high uptake efficiency in oligotrophic waters. In general, however, NO_3^- assimilation rates were an order of magnitude lower than those reported in other studies (Cavagna *et al.*, 2015; Raes *et al.*, 2015). Cavagna *et al.* (2015) report rates around $29 - 1900 \text{ nmol L}^{-1} \text{ d}^{-1}$ in the adjacent Kerguelen region in spring. Raes *et al.* (2015) report NO_3^- assimilation rates of around $43.2 - 84 \text{ nmol L}^{-1} \text{ d}^{-1}$ in the south-eastern IO in middle

to late winter. Although these studies are at different times of year, we consider that our data do show exceptionally low rates.

NH₄⁺ assimilation

NH₄⁺ uptake provides an important N source for primary production. Generally, NH₄⁺ assimilation rates have been observed to follow the same trend as C fixation in this region (Cavagna et al., 2015). However, Cavagna et al (2015) also report high nitrification rates, which indicate potential competition between autotrophs and nitrifiers. Assuming a high conversion rate of NH₄⁺ to NO₃⁻, classical separation between NO₃⁻ and NH₄⁺ (*f*-ratio; Dugdale & Goering 1967) is not applicable for these regions (Raes *et al.*, 2015). Since the [eastern] IO is considered to be nitrogen depleted (relative to phosphate and silicate; (Raes *et al.*, 2015)) other sources than NO₃⁻ and NH₄⁺, through regeneration and microbial recycling, are needed to support primary productivity. NH₄⁺ assimilation rates in our work were in the same range as reported by Cavagna et al (2014), who indicated that NH₄⁺ assimilation rates were relatively constant throughout the area around Kerguelen Island. In our data set, NH₄⁺ assimilation rates were also relatively constant throughout the whole sampling area, though they had no direct correlation with primary production.

5. Conclusion

Our data show that the water masses in the Southern Indian Ocean (IO) and the IO sector of the Southern Ocean separate not only physically but also biologically. The IO is a warm oligotrophic environment dominated by the known ubiquitous cyanobacterial species *Prochlorococcus* and *Synechococcus*. However, these are not dominant in the cold- water of the Antarctic Circumpolar Current (ACC) and Polar Front (PF). The latter two water masses are dominated by diatoms and pico-eukaryotes. In areas of relatively high diatom concentrations we found prokaryotes of the order Flavobacteria which have been described to co-occur with diatoms. We found a great variety of autotrophic pigments and highest prokaryotic diversity in the mixed water of the IO and ACC. We also measured relatively high C fixation rates for the same area, suggesting that both primary production itself, and community composition of primary producers can be a source for great microbial diversity. Interestingly, cell specific C uptake did not show a trend between different water masses, suggesting top- down control rather than bottom up control of productivity.

In contrast to previous studies, which suggested N₂ fixation exclusively to oligotrophic warm waters, we could measure N₂ fixation throughout the whole sampling area to 56°S. However, the natural abundance of $\delta^{15}\text{N}$ suggests that the relative importance of N₂ fixation to the total N pool potentially varies strongly between water masses. Our data contributes to an understanding of N₂ fixation in high latitude waters. Supporting and understanding of the factors driving diazotroph community and activity.

We observed a high variance between within-station replicates of C- and N₂ fixation measurements as well as measurements of N assimilation. Among other interpretations, this suggests sub-mesoscale dynamics and potential small-scale differences in biochemical conditions. Our observations point out the importance of high resolution (i.e., sub-mesoscale and smaller) *in situ* studies in combination with remote- sensing techniques, to be able to fully understand the scale of variation in ocean dynamics. Absolute C fixation rates, and microbial community composition, have significant impact on C and N cycles. Understanding biochemical and biological processes supports our ability to further understand C and N fluxes to be able to predict and model future climate change scenarios.

Acknowledgement

I would first like to thank Eric J. Raes who gave me the opportunity to pursue my interests in oceanography and biodiversity. His supervision allowed me both to extend my knowledge and to think in a creative and scientific way. For reviewing my thesis, I am very thankful to Anya Waite and Bernhard Fuchs. I am especially grateful to my supervisor Anya Waite for the opportunity to pursue my research in her group, for supervising my thesis and providing helpful comments on the manuscripts. Your knowledge and enthusiasm for science is very impressive, and our discussions were always interesting as well as valuable. I would also like to thank Allison Fong for her open doors and her helpful technical and scientific comments on this thesis. For help and advice in terms of sequencing techniques I would like to thank Vladimir Benes and his entire team from the EMBL. Thanks to Claire Io Monaco and Nicolas Metzl as well as the captain and crew of the Marion Dufresne. Thanks to Gaute Lavik and the whole Biogeography group from the MPI Bremen for the guidance and support using the MIMS analyser. Many thanks to Sarah Weil and Christine Rundt for their thorough sampling efforts.

I am thankful to a number of colleagues from the AWI, to Susanne Spahic, Kerstin Oetjen and Swantje Rogge for their time and help in all kind of problems I faced in the last six months. Thanks to Sinhue Torres-Valdes and Laura Wischnewski for their help with the nutrient analysis. For supervision in the HPLC lab, I am thankful to Sandra Murawski.

I also want to thank Alejandra Mera for her valuable comments on this thesis. Many thanks to the Marmic program and, in particular, to my classmates David Benito Merino and Matthew Schechter for their help, comments, discussions, unhealthy amount of coffee and fun time making grey (Bremen-)days brighter and cheerful. Last but not least, I want to thank my family, my friends and my partner, Jerome Kallisch, for their encouragement, smiles and support during this whole master program.

References

- Aiken, J., Pradhan, Y., Barlow, R., Lavender, S., Poulton, A., Holligan, P. and Hardman-mountford, N. (2009) 'Phytoplankton pigments and functional types in the Atlantic Ocean : A decadal assessment , 1995 – 2005', *Deep-Sea Research Part II: Topical Studies in Oceanography*, 56, pp. 899–917. doi: 10.1016/j.dsr2.2008.09.017.
- Alexander, D., Ameer, A., Rupakjyoti, B., Fernando, Y. J. S. N., Forbes, V. L., Gordon, S., Hayward, D. L. O., Hughes, J., Hartley, J., Hanasz, P., Jacob, J. T., Luke, L. G., O'Loughlin, C., DeSilva-Ranasinghe, S., Robinson, D. A. and Thomas, J. (2012) 'Indian Ocean : A Sea of Uncertainty', in *Independet Strategic Analysis of Australia's Global Interests*. Perth, Australia.
- Armstrong, F. A. J. (1951) 'The determination of silicate in sea water', *Journal of the Marine Biological Association of the United Kingdom*, 30(1), pp. 149–160. doi: 10.1017/S0025315400012649.
- Arrigo, K. R. (1999) 'Phytoplankton community structure and the drawdown of nutrients and CO₂ in the Southern Ocean', *Science*, 283(5400), pp. 365–367. doi: 10.1126/science.283.5400.365.
- Arrigo, K. R. (2005) 'Marine microorganisms and global nutrient cycles', *Nature*, 437(7057), p. 349. doi: 10.1038/nature04158.
- Azam, F., Fenchel, T., Field, J. G., Gray, J. S., Meyer - Reil, L. A. and Thingstad, F. (1983) 'The Ecological Role of Water - Column Microbes in the Sea', *Marine Ecology Progress Series*, pp. 257–263. doi: 10.3354/meps010257.
- de Baar, H. J. W., Bathmann, U., Smetacek, V., Löscher, B. M. and Veth, C. (1995) 'Importance of iron for plankton blooms and carbon dioxide drawdown in the Southern Ocean', *Nature*, pp. 412–415. doi: 10.1038/373412a0.
- Baltar, F. and Arístegui, J. (2017) 'Fronts at the Surface Ocean Can Shape Distinct Regions of Microbial Activity and Community Assemblages Down to the Bathypelagic Zone: The Azores Front as a Case Study', *Frontiers in Marine Science*, 4(August), pp. 1–13. doi: 10.3389/fmars.2017.00252.
- Barcelos e Ramos, J., Biswas, H., Schulz, K. G., LaRoche, J. and Riebesell, U. (2007) 'Effect of

- rising atmospheric carbon dioxide on the marine nitrogen fixer *Trichodesmium*', *Global Biogeochemical Cycles*, 21(2), pp. 1–6. doi: 10.1029/2006GB002898.
- Beaufort, L. (1997) 'Insolation Cycles as a Major Control of Equatorial Indian Ocean Primary Production', *Science*, 278(5342), pp. 1451–1454. doi: 10.1126/science.278.5342.1451.
- Benavides, M., Agawin, N. S. R., Arístegui, J., Peene, J. and Stal, L. J. (2013) 'Dissolved organic nitrogen and carbon release by a marine unicellular diazotrophic cyanobacterium', *Aquatic Microbial Ecology*, 69(Sellner 1997), pp. 69–80. doi: 10.3354/ame01621.
- Bentzon-Tilia, M., Traving, S. J., Mantikci, M., Knudsen-Leerbeck, H., Hansen, J. L. S., Markager, S. and Riemann, L. (2015) 'Significant N₂ fixation by heterotrophs, photoheterotrophs and heterocystous cyanobacteria in two temperate estuaries', *ISME Journal*, 9(2), pp. 273–285. doi: 10.1038/ismej.2014.119.
- Berges, J. A. and Mulholland, M. R. (2008) 'Enzymes and Nitrogen Cycling', in Capone, D. G., Bronk, D. A., Mulholland, M. R., and Carpenter, E. J. (eds) *Nitrogen in the Marine Environment*. 2nd edn. Elsevier, pp. 1385–1444. doi: 10.1016/B978-0-12-372522-6.00032-3.
- Blain, S., Capparos, J., Guéneuguès, A., Obernosterer, I. and Oriol, L. (2015) 'Distributions and stoichiometry of dissolved nitrogen and phosphorus in the iron-fertilized region near Kerguelen (Southern Ocean)', *Biogeosciences*, 12, pp. 623–635. doi: 10.5194/bg-12-623-2015.
- Blain, S., Quéguiner, B., Armand, L., Belviso, S., Bombled, B., Bopp, L., Bowie, A., Brunet, C., Brussaard, C., Carlotti, F., Christaki, U., Corbière, A., Durand, I., Ebersbach, F., Fuda, J.-L., Garcia, N., Gerringa, L., Griffiths, B., Guigue, C., Guillerm, C., Jacquet, S., Jeandel, C., Laan, P., Lefèvre, D., Lo Monaco, C., Malits, A., Mosseri, J., Obernosterer, I., Park, Y.-H., Picheral, M., Pondaven, P., Remenyi, T., Sandroni, V., Sarthou, G., Savoye, N., Scouarnec, L., Souhaut, M., Thuiller, D., Timmermans, K., Trull, T., Uitz, J., van Beek, P., Veldhuis, M., Vincent, D., Viollier, E., Vong, L. and Wagener, T. (2007) 'Effect of natural iron fertilization on carbon sequestration in the Southern Ocean', *Nature*, 446(7139), pp. 1070–1074. doi: 10.1038/nature05700.
- Blain, S., Sarthou, G. and Laan, P. (2008) 'Distribution of dissolved iron during the natural iron-fertilization experiment KEOPS (Kerguelen Plateau, Southern Ocean)', *Deep-Sea Research Part II: Topical Studies in Oceanography*, 55(5–7), pp. 594–605. doi:

10.1016/j.dsr2.2007.12.028.

Boissin, E., Hoareau, T. B., Paulay, G. and Bruggemann, J. H. (2017) 'DNA barcoding of reef brittle stars (Ophiuroidea, Echinodermata) from the southwestern Indian Ocean evolutionary hot spot of biodiversity', *Ecology and Evolution*, 7(24), pp. 11197–11203. doi: 10.1002/ece3.3554.

Bolger, A. M., Lohse, M. and Usadel, B. (2014) 'Trimmomatic: A flexible trimmer for Illumina sequence data', *Bioinformatics*, 30(15), pp. 2114–2120. doi: 10.1093/bioinformatics/btu170.

Bowie, A. R., Van Der Merwe, P., Qu  rou  , F., Trull, T., Fourquez, M., Planchon, F., Sarthou, G., Chever, F., Townsend, A. T., Obernosterer, I., Sall  e, J. B. and Blain, S. (2015) 'Iron budgets for three distinct biogeochemical sites around the Kerguelen Archipelago (Southern Ocean) during the natural fertilisation study, KEOPS-2', *Biogeosciences*, 12(14), pp. 4421–4445. doi: 10.5194/bg-12-4421-2015.

Boyd, P. W., Strzepek, R., Fu, F. and Hutchins, D. A. (2010) 'Environmental control of open-ocean phytoplankton groups : Now and in the future', *Limnology and Oceanography*, 55(3), pp. 1353–1376. doi: 10.4319/lo.2010.55.3.1353.

Boyd, P. W., Watson, A. J., Law, C. S., Abraham, E. R., Trull, T., Murdoch, R., Bakker, D. C. E., Bowie, A. R., Buesseler, K. O., Chang, H., Charette, M., Croot, P., Downing, K., Frew, R., Gall, M., Hadfield, M., Hall, J., Harvey, M., Jameson, G., LaRoche, J., Liddicoat, M., Ling, R., Maldonado, M. T., McKay, R. M., Nodder, S., Pickmere, S., Pridmore, R., Rintoul, S., Safi, K., Sutton, P., Strzepek, R., Tanneberger, K., Turner, S., Waite, A. and Zeldis, J. (2000) 'A mesoscale phytoplankton bloom in the polar Southern Ocean stimulated by iron fertilization', *Nature*, 407(6805), pp. 695–702. doi: 10.1038/35037500.

Boynton, W. R., Kemp, W. M. and Keefe, C. W. (1982) 'A comparative analysis of nutrients and other factors influencing estuarine phytoplankton production', *Estuarine comparisons*, pp. 69–90.

Breitbarth, E., Oschlies, A., Laroche, J., Breitbarth, E., Oschlies, A. and Physiological, J. L. (2007) 'Physiological constraints on the global distribution of *Trichodesmium* ? effect of temperature on diazotrophy', *Biogeosciences, European Geosciences Union*, 4(1), pp. 53–61.

Brewin, R. J. W., Sathyendranath, S., Hirata, T., Lavender, S. J., Barciela, R. M. and Hardman-

- mountford, N. J. (2010) 'A three-component model of phytoplankton size class for the Atlantic Ocean', *Ecological Modelling*. Elsevier B.V., 221(11), pp. 1472–1483. doi: 10.1016/j.ecolmodel.2010.02.014.
- Brown, S. L. and Landry, M. R. (2001) 'Mesoscale variability in biological community structure and biomass in the Antarctic Polar Front region at 170°W during austral spring 1997', *Journal of Geophysical Research: Oceans*, 106(C7), pp. 13917–13930. doi: 10.1029/1999JC000188.
- Capone, D. G. (1997) 'Trichodesmium, a Globally Significant Marine Cyanobacterium', *Science*, 276(5316), pp. 1221–1229. doi: 10.1126/science.276.5316.1221.
- Capone, D. G., Burns, J. A., Montoya, J. P., Subramaniam, A., Mahaffey, C., Gunderson, T., Michaels, A. F. and Carpenter, E. J. (2005) 'Nitrogen fixation by *Trichodesmium* spp.: An important source of new nitrogen to the tropical and subtropical North Atlantic Ocean', *Global Biogeochemical Cycles*, 19(2), pp. 1–17. doi: 10.1029/2004GB002331.
- Capotondi, A., Alexander, M. A., Bond, N. A., Curchitser, E. N. and Scott, J. D. (2012) 'Enhanced upper ocean stratification with climate change in the CMIP3 models', *Journal of Geophysical Research: Oceans*, 117(4), pp. 1–23. doi: 10.1029/2011JC007409.
- Carpenter, E. J., Montoya, J. P., Burns, J., Mulholland, M. R., Subramaniam, A. and Capone, D. G. (1999) 'Extensive bloom of a N₂-fixing diatom/cyanobacterial association in the tropical Atlantic Ocean', *Marine Ecology Progress Series*, 185(1977), pp. 273–283. doi: 10.3354/meps185273.
- Cavagna, A. J., Fripiat, F., Elskens, M., Mangion, P., Chirurgien, L., Closset, I., Lasbleiz, M., Florez-Leiva, L., Cardinal, D., Leblanc, K., Fernandez, C., Lefèvre, D., Oriol, L., Blain, S., Quéguiner, B. and Dehairs, F. (2015) 'Production regime and associated N cycling in the vicinity of Kerguelen Island, Southern Ocean', *Biogeosciences*, 12(21), pp. 6515–6528. doi: 10.5194/bg-12-6515-2015.
- Christaki, U., Lefèvre, D., Georges, C., Colombet, J., Catala, P., Courties, C., Sime-Ngando, T., Blain, S. and Obernosterer, I. (2014) 'Microbial food web dynamics during spring phytoplankton blooms in the naturally iron-fertilized Kerguelen area (Southern Ocean)', *Biogeosciences*, 11(23), pp. 6739–6753. doi: 10.5194/bg-11-6739-2014.

- Codispoti, L. A., Brandes, J. A., Christensen, J. P., Devol, A. H., Naqvi, S. W. A., Paerl, H. W. and Yoshinari, T. (2001) 'The oceanic fixed nitrogen and nitrous oxide budgets: Moving targets as we enter the anthropocene?', *Scientia Marina*, 65(S2), pp. 85–105. doi: 10.3989/scimar.2001.65s285.
- Crawford, D. W., Wyatt, S. N., Wrohan, I. A., Cefarelli, A. O., Giesbrecht, K. E., Kelly, B. and Varela, D. E. (2015) 'Low particulate carbon to nitrogen ratios in marine surface waters of the Arctic', *Global Biogeochemical Cycles*, 29(12), pp. 2021–2033. doi: 10.1002/2015GB005200.Received.
- Dafner, E. V. and Mordasova, N. V. (1994) 'Influence of biotic factors on the hydrochemical structure of surface water in the Polar Frontal Zone of the Atlantic Antarctic', *Marine Chemistry*, 45(1–2), pp. 137–148. doi: 10.1016/0304-4203(94)90098-1.
- Edwards, J. L., Smith, D. L., Connolly, J., McDonald, J. E., Cox, M. J., Joint, I., Edwards, C. and McCarthy, A. J. (2010) 'Identification of carbohydrate metabolism genes in the metagenome of a marine biofilm community shown to be dominated by Gammaproteobacteria and Bacteroidetes', *Genes*, 1(3), pp. 371–384. doi: 10.3390/genes1030371.
- Falkowski, P. G. (1997) 'Evolution of the nitrogen cycle and its influence on the biological sequestration of CO₂ in the ocean', *Nature*, 387(6630), pp. 272–275. doi: 10.1038/387272a0.
- Farnelid, H., Andersson, A. F., Bertilsson, S., Al-Soud, W. A., Hansen, L. H., Sørensen, S., Steward, G. F., Hagström, Å. and Riemann, L. (2011) 'Nitrogenase gene amplicons from global marine surface waters are dominated by genes of non-cyanobacteria', *PLoS ONE*, 6(4), p. e19223. doi: 10.1371/journal.pone.0019223.
- Fawcett, S. E., Lomas, M. W., Ward, B. B. and Sigman, D. M. (2014) 'Global Biogeochemical Cycles production in the Sargasso Sea', *Global Biogeochemical Cycles*, 28, pp. 86–102. doi: 10.1002/2013GB004579.Received.
- Fernández-Méndez, M., Turk-Kubo, K. A., Buttigieg, P. L., Rapp, J. Z., Krumpen, T., Zehr, J. P. and Boetius, A. (2016) 'Diazotroph diversity in the sea ice, melt ponds, and surface waters of the eurasian basin of the Central Arctic Ocean', *Frontiers in Microbiology*, 7(NOV), pp. 1–18. doi: 10.3389/fmicb.2016.01884.
- Field, C. B., Behrenfeld, M. J., Randerson, J. T., Falkowski, P., Field, C. B., Behrenfeld, M. J.

- and Randerson, J. T. (1998) 'Primary Production of the Biosphere : Integrating Terrestrial and Oceanic Components', 281(5374), pp. 237–240. Available at: <http://www.ncbi.nlm.nih.gov/pubmed/9660741>.
- Fu, F. X. and Bell, P. R. F. (2003) 'Factors affecting N₂ fixation by the cyanobacterium *Trichodesmium* sp. GBRTLI101', *FEMS Microbiology Ecology*, 45(2), pp. 203–209. doi: 10.1016/S0168-6496(03)00157-0.
- Fuhrman, J. A., Steele, J. A., Hewson, I., Schwalbach, M. S., Brown, M. V., Green, J. L. and Brown, J. H. (2008) 'A latitudinal diversity gradient in planktonic marine bacteria', *Proceedings of the National Academy of Sciences*, 105(22), pp. 7774–8. doi: 10.1073/pnas.0803070105.
- Garcia, N. S., Fu, F., Breene, C. L., Bernhardt, P. W., Mulholland, M. R., Sohm, J. A. and Hutchins, D. A. (2011) 'Interactive Effects Of Irradiance and CO₂ on CO₂ Fixation and N₂ Fixation in the Diazotroph *Trichodesmium Erythraeum* (Cyanobacteria)', *Journal of Phycology*, 47, pp. 1292–1303. doi: 10.1111/j.1529-8817.2011.01078.x.
- Giovannoni, S. J. (2017) 'SAR11 Bacteria: The Most Abundant Plankton in the Oceans', *Annual Review of Marine Science*, 9(1), pp. 231–255. doi: 10.1146/annurev-marine-010814-015934.
- Goering, J. J., Dugdale, C. and Menzel, D. W. (1966) 'Estimates of in situ rates of nitrogen uptake by *Trichodesmium* sp. in the tropical Atlantic Ocean', *Limnology & Oceanography*, 11, pp. 614–620. doi: 10.4319/lo.1966.11.4.0614.
- Goeyens, L., Semeneh, M., Baumann, M. E. M., Elskens, M., Shopova, D. and Dehairs, F. (1998) 'Phytoplanktonic nutrient utilisation and nutrient signature in the Southern Ocean', *Journal of Marine Systems*, 17(1–4), pp. 143–157. doi: 10.1016/S0924-7963(98)00035-9.
- Gómez-Pereira, P. R., Schüler, M., Fuchs, B. M., Bennke, C., Teeling, H., Waldmann, J., Richter, M., Barbe, V., Bataille, E., Glöckner, F. O. and Amann, R. (2012) 'Genomic content of uncultured Bacteroidetes from contrasting oceanic provinces in the North Atlantic Ocean', *Environmental Microbiology*, 14(1), pp. 52–66. doi: 10.1111/j.1462-2920.2011.02555.x.
- González, M. L., Molina, V., Oriol, L. and Cavagna, A. J. (2014) 'Nitrogen fixation in the Southern Ocean : a case of study of the Fe-fertilized Kerguelen region (KEOPS II cruise)',

- Biogeosciences Discussions*, 11, pp. 17151–17185. doi: 10.5194/bgd-11-17151-2014.
- Gradoville, M. R., Bombar, D., Crump, B. C., Letelier, R. M., Zehr, J. P. and White, A. E. (2017) 'Diversity and activity of nitrogen-fixing communities across ocean basins', *Limnology and Oceanography*, 62(5), pp. 1895–1909. doi: 10.1002/lno.10542.
- Großkopf, T., Mohr, W., Baustian, T., Schunck, H., Gill, D., Kuypers, M. M. M., Lavik, G., Schmitz, R. A., Wallace, D. W. R. and Laroche, J. (2012) 'Doubling of marine dinitrogen-fixation rates based on direct measurements', *Nature*. Nature Publishing Group, 488(7411), pp. 361–364. doi: 10.1038/nature11338.
- Gruber, N. (2008) *The Marine Nitrogen Cycle : Overview and Challenges*.
- Gruber, N. and Galloway, J. N. (2008) 'An Earth-system perspective of the global nitrogen cycle', *Nature*, 451(7176), pp. 293–296. doi: 10.1038/nature06592.
- Gruber, N. and Sarmiento, J. L. (1997) 'Global patterns of marine nitrogen fixation and denitrification', *Global Biogeochemical Cycles*, 11(2), pp. 235–266.
- Hart, T. J. (1942) 'Phytoplankton periodicity in the Antarctic surface waters', *Discovery Rep.*, 21, pp. 261–356.
- Hirata, T., Brewin, R. J. W., Aiken, J., Barlow, R., Suzuki, K. and Isada, T. (2011) 'Synoptic relationships between surface Chlorophyll- a and diagnostic pigments specific to phytoplankton functional types', *Biogeosciences*, 8, pp. 311–327. doi: 10.5194/bg-8-311-2011.
- Hoegh-Guldberg, O. and Bruno, J. F. (2010) 'The Impact of Climate Change on the World's Marine Ecosystems', *Science*, 328, pp. 1523–1528.
- Hood, R. R., Bange, H. W., Beal, L., Beckley, L., Burkill, P., Cowie, G. L., D'Adamo, N., Ganssen, G., Hendon, H., Hermes, J., Honda, M., McPhaden, M., Roberts, M., Singh, S., Urban, E. and Yu, W. (2015) 'SECOND INTERNATIONAL INDIAN OCEAN EXPEDITION (IIOE-2) A Basin-Wide Research Program', *Scientific Committee on Oceanic Research, Newark, Delaware, USA*.
- Hood, R. R., Coles, V. J. and Capone, D. G. (2004) 'Modeling the distribution of Trichodesmium and nitrogen fixation in the Atlantic Ocean', *Journal of Geophysical Research C: Oceans*, 109(6), pp. 1–25. doi: 10.1029/2002JC001753.

- Hood, R. R., Urban, E. R., McPhaden, M. J., Su, D. and Raes, E. (2016) 'The 2nd International Indian Ocean Expedition (IIOE-2): Motivating New Exploration in a Poorly Understood Basin', *Limnology and Oceanography Bulletin*, 25(4), pp. 117–124. doi: 10.1002/lob.10149.
- Huston, M. (1979) 'A General Hypothesis of Species Diversity', *The American Naturalist*, 113(1), pp. 81–101.
- Hutchins, D. A., Fu, F.-X., Zhang, Y., Warner, M. E., Feng, Y., Portune, K., Bernhardt, P. W. and Mulholland, M. R. (2007) 'CO₂ control of Trichodesmium N₂ fixation, photosynthesis, growth rates, and elemental ratios: Implications for past, present, and future ocean biogeochemistry', *Limnology and Oceanography*, 52(4), pp. 1293–1304. doi: 10.4319/lo.2007.52.4.1293.
- Hutchins, D. A., Walworth, N. G., Webb, E. A., Saito, M. A., Moran, D., McIlvin, M. R., Gale, J. and Fu, F. X. (2015) 'Irreversibly increased nitrogen fixation in Trichodesmium experimentally adapted to elevated carbon dioxide', *Nature Communications*. Nature Publishing Group, 6, pp. 1–7. doi: 10.1038/ncomms9155.
- IPCC (2014) *Climate Change 2014: Synthesis Report. Contribution of Working Groups I, II and III to the Fifth Assessment Report of the Intergovernmental Panel on Climate Change [Core Writing Team, R.K. Pachauri and L.A. Meyer (eds.)]*. Geneva, Switzerland.
- Jochem, F. J., Mathot, S. and Quéguiner, B. (1995) 'Size-fractionated primary production in the open Southern Ocean in austral spring', *Polar Biology*, 15(6), pp. 381–392. doi: 10.1007/BF00239714.
- Johnson, Z. I., Zinser, E. R., Coe, A., McNulty, N. P., Malcolm, E. S., Chisholm, S. W., Woodward, E. M. S. and Chisholm, S. W. (2006) 'Niche Partitioning Among Prochlorococcus Ecotypes Along Ocean-Scale Environmental Gradients', *Science*, 311(March), pp. 1737–1740. doi: 10.1126/science.1118052.
- Jongsun Kim and D. C. Rees (1992) 'Structural Models for the Metal Centers in the Nitrogenase Molybdenum-Iron protein', *Science, New Series*, 257(5077), pp. 1677–1682. doi: 10.1126/science.1529354.
- Karl, D., Letelier, R., Tupas, L., Dore, J., Christian, J. and Hebel, D. (1997) 'The role of nitrogen fixation in biogeochemical cycling in the subtropical North Pacific Ocean', *Nature*, 388(6642),

pp. 533–538. doi: 10.1038/41474.

Karl, D., Michaels, A., Bergman, B., Capone, D. G., Carpenter, E. J., Letelier, R., Lipschultz, F., Paerl, H., Sigman, D. and Stal, L. (2002) 'Dinitrogen fixation in the world's oceans', *Biogeochemistry*, 57–58, pp. 47–98. doi: 10.1023/A:1015798105851.

Kilias, E., Wolf, C., Nöthig, E. M., Peeken, I. and Metfies, K. (2013) 'Protist distribution in the Western Fram Strait in summer 2010 based on 454-pyrosequencing of 18S rDNA', *Journal of Phycology*, 49(5), pp. 996–1010. doi: 10.1111/jpy.12109.

Klawonn, I., Lavik, G., Böning, P., Marchant, H. K., Dekaezemacker, J., Mohr, W. and Ploug, H. (2015) 'Simple approach for the preparation of 15-15N₂-enriched water for nitrogen fixation assessments: Evaluation, application and recommendations', *Frontiers in Microbiology*, 6(AUG), pp. 1–11. doi: 10.3389/fmicb.2015.00769.

Knap, A., Michaels, A., Close, A., Ducklow, H. and Dickson, A. (1996) 'Protocols for the Joint Global Ocean Flux Study (JGFOS) Core Measurements', *JGOFs Reoprt Nr. 19, vi+170 pp*, (Reprint of IOC MAnnuals and Guides 29, UNESCO 1994), p. 198. doi: 10013/epic.27912.

Kustka, A. B., Carpenter, E. J. and Sanudo-Wilhelmy, S. (2002) 'Iron and marine fixation: progress and future directions', *Research in Microbiology*, 153, pp. 255–262.

Laubscher, R. K., Perissinotto, R. and McQuaid, C. D. (1993) 'Phytoplankton Production and Biomass at Frontal Zones in the Atlantic Sector of the Southern-Ocean', *Polar Biology*, 13(7), pp. 471–481.

Levitan, O., Rosenberg, G., Setlik, I., Setlikova, E., Grigel, J., Klepetar, J., Prasil, O. and Berman-Frank, I. (2007) 'Elevated CO₂ enhances nitrogen fixation and growth in the marine cyanobacterium *Trichodesmium*', *Global Change Biology*, 13(2), pp. 531–538. doi: 10.1111/j.1365-2486.2006.01314.x.

Levitus, S., Conkright, M. E., Reid, J. L., Najjar, R. G. and Mantyla, A. (1993) 'Distribution of nitrate, phosphate and silicate in the world oceans', *Progress in Oceanography*, 31(3), pp. 245–273. doi: 10.1016/0079-6611(93)90003-V.

Loescher, C. R., Großkopf, T., Desai, F. D., Gill, D., Schunck, H., Croot, P. L., Schlosser, C., Neulinger, S. C., Pinnow, N., Lavik, G., Kuypers, M. M. M., Laroche, J. and Schmitz, R. A. (2014) 'Facets of diazotrophy in the oxygen minimum zone waters off Peru', *ISME Journal*,

8(11), pp. 2180–2192. doi: 10.1038/ismej.2014.71.

Luo, Y.-W., Doney, S. C., Anderson, L. A., Benavides, M., Bode, A., Bonnet, S., Capone, D. G., Carpenter, E. J., Chen, Y. L., Church, M. J., Dore, J. E., Foster, R. A., Furuya, K., Gundersen, K., Hynes, A. M., Karl, D. M., Kitajima, S., Langlois, R. J., Laroche, J., Letelier, R. M., Moisander, P. H., Moore, C. M., Mulholland, M. R., Needoba, J. A., Orcutt, K. M., Poulton, A. J., Rahav, E., Raimbault, P., Rees, A. P., Riemann, L., Shiozaki, T., Subramaniam, A., Tyrrell, T., Varela, M., Villareal, T. A., Webb, E. A., White, A. E., Wu, J., Zehr, J. P., Hole, W., Hole, W., Hole, W., Hole, W., Palmas, L., Canaria, D. G., Mina, T., Angeles, L. and Vigo, U. De (2012) 'Database of diazotrophs in global ocean: abundance, biomass and nitrogen fixation rates', *Earth System Science Data*, 4, pp. 47–73. doi: 10.5194/essd-4-47-2012.

Lutjeharms, J. R. E., Walters, N. M. and Allanson, B. R. (1985) 'Oceanic frontal systems and biological enhancement', in *Antarctic Nutrient Cycles and Food Webs*, pp. 11–21.

Mahé, F., Rognes, T., Quince, C., de Vargas, C. and Dunthorn, M. (2014) 'Swarm: robust and fast clustering method for amplicon-based studies', *PeerJ*, 2, p. e593. doi: 10.7717/peerj.593.

Martin, J. H. (1992) 'Iron as a limiting factor in oceanic productivity', in Falkowski, P. G. and Woodhead, A. D. (eds) *Primary Productivity and Biogeochemical Cycles in the Sea*. New York: Springer, pp. 123–137.

Martin, M. (2011) 'Cutadapt removes adapter sequences from high-throughput sequencing reads', *EMBnet.journal*, 17(1), p. 10. doi: 10.14806/ej.17.1.200.

Martínez-Pérez, C., Mohr, W., Löscher, C. R., Dekaezemacker, J., Littmann, S., Yilmaz, P., Lehnen, N., Fuchs, B. M., Lavik, G., Schmitz, R. A., LaRoche, J. and Kuypers, M. M. M. (2016) 'The small unicellular diazotrophic symbiont, UCYN-A, is a key player in the marine nitrogen cycle', *Nature Microbiology*. Nature Publishing Group, 1(11), pp. 1–7. doi: 10.1038/nmicrobiol.2016.163.

Martiny, A. C., Vrugt, J. A., Primeau, F. W. and Lomas, M. W. (2013) 'Regional variation in the particulate organic carbon to nitrogen ratio in the surface ocean', *Global Biogeochemical Cycles*, 27(3), pp. 723–731. doi: 10.1002/gbc.20061.

Mather, R. L., Reynolds, S. E., Wolff, G. A., Williams, R. G., Torres-Valdes, S., Woodward, E. M. S., Landolfi, A., Pan, X., Sanders, R. and Achterberg, E. P. (2008) 'Phosphorus cycling in the

- North and South Atlantic Ocean subtropical gyres', *Nature Geoscience*, 1(7), pp. 439–443. doi: 10.1038/ngeo232.
- McCarthy, J. J. (1981) 'Kinetics of nutrient utilization', *Canadian Bulletin of Fisheries and Aquatic Sciences*, 210, pp. 211–233.
- Mehta, M. P., Butterfield, D. a and Baross, J. a (2003) 'Phylogenetic Diversity of Nitrogenase (nifH) Genes in Deep-Sea and Hydrothermal Vent Environments of the Juan de Fuca Ridge', *Applied and environmental microbiology*, 69(2), pp. 960–970. doi: 10.1128/AEM.69.2.960.
- Menge, B. A. and Sutherland, J. P. (1976) 'Species Diversity Gradients : Synthesis of the Roles of Predation , Competition , and Temporal Heterogeneity', *The American Naturalist*, 110(973), pp. 351–369.
- Messer, L. F., Doubell, M., Jeffries, T. C., Brown, M. V. and Seymour, J. R. (2015) 'Prokaryotic and diazotrophic population dynamics within a large oligotrophic inverse estuary', *Aquatic Microbial Ecology*, 74(1), pp. 1–15. doi: 10.3354/ame01726.
- Michaels, A. F. and Silver, M. W. (1988) 'Primary production, sinking fluxes and the microbial food web', *Deep-Sea Research*, 35(4), pp. 473–490.
- Mohr, W., Großkopf, T., Wallace, D. W. R. and LaRoche, J. (2010) 'Methodological underestimation of oceanic nitrogen fixation rates', *PLoS ONE*, 5(9), pp. 1–7. doi: 10.1371/journal.pone.0012583.
- Moisander, P. H., Beinart, R. A., Hewson, I., White, A. E., Johnson, K. S., Carlson, C. A., Montoya, J. P. and Zehr, J. P. (2010) 'Unicellular Cyanobacterial Distributions Broaden the Oceanic N₂ Fixation Domain', *Science*, 327(5972), pp. 1512–1514. doi: 10.1126/science.1185468.
- Mongin, M., Molina, E. and Trull, T. W. (2008) 'Seasonality and scale of the Kerguelen plateau phytoplankton bloom: A remote sensing and modeling analysis of the influence of natural iron fertilization in the Southern Ocean', *Deep-Sea Research Part II: Topical Studies in Oceanography*, 55(5–7), pp. 880–892. doi: 10.1016/j.dsr2.2007.12.039.
- Montoya, J. P. (2007) 'Natural abundancce of 15N in marine planktonic ecosystems', in MICHENER, R. and LAJTHA, K. (eds) *Stable isotopes in ecology and environmental science*. 2nd edn. Blackwell publishing, pp. 176–201. doi: 10.1899/0887-3593-028.002.0516.

- Montoya, J. P., Carpenter, E. J. and Capone, D. G. (2002) 'Nitrogen fixation and nitrogen isotop abundance in zooplankton of the oligotrophic North Atlantic', *Limnology & Oceanography*, 47(6), pp. 1617–1628. doi: 10.4319/lo.2002.47.6.1617.
- Montoya, J. P., Holl, C. M., Zehr, J. P., Hansen, A., Villareal, T. A. and Capone, D. G. (2004) 'High rates of N₂ fixation by unicellular diazotrophs in the oligotrophic Pacific Ocean', 430(August), pp. 1027–1031. doi: 10.1038/nature02744.1.
- Montoya, J. P., Voss, M. and Capone, D. G. (2007) 'Spatial variation in N₂ -fixation rate and diazotroph activity in the Tropical Atlantic', *Biogeosciences*, 4, pp. 369–376. doi: 10.5194/bg-4-369-2007.
- Montoya, J. P., Voss, M., Kahler, P. and Capone, D. G. (1996) 'A Simple , High-Precision , High-Sensitivity Tracer Assay for N₂ Fixation', *Applied and Environmental Microbiology*, 62(3), pp. 986–993.
- Moore, J. K. and Abbott, M. R. (2002) 'Surface chlorophyll concentrations in relation to the Antarctic Polar Front: Seasonal and spatial patterns from satellite observations', *Journal of Marine Systems*, 37(1–3), pp. 69–86. doi: 10.1016/S0924-7963(02)00196-3.
- Moore, J. K. and Doney, S. C. (2007) 'Iron availability limits the ocean nitrogen inventory stabilizing feedbacks between marine denitrification and nitrogen fixation', *Global Biogeochemical Cycles*, 21(2), pp. 1–12. doi: 10.1029/2006GB002762.
- Moore, J. K., Doney, S. C., Glover, D. M. and Fung, I. Y. (2002) 'Iron cycling and nutrient-limitation patterns in surface waters of the world ocean', *Deep-Sea Research Part II: Topical Studies in Oceanography*, 49(1–3), pp. 463–507. doi: 10.1016/S0967-0645(01)00109-6.
- Moutin, T., Karl, D. M., Duhamel, S., Rimmelin, P., Raimbault, P., Van Mooy, B. A. S. and Claustre, H. (2007) 'Phosphate availability and the ultimate control of new nitrogen input by nitrogen fixation in the tropical Pacific Ocean', *Biogeosciences Discussions*, 4(4), pp. 2407–2440. doi: 10.5194/bgd-4-2407-2007.
- Murphy, J. and Riley, J. (1962) 'A modified single solution method for the determination of phosphate in natural waters', *Analytical Chemistry ACTA*, 27, pp. 31–36. doi: 10.1016/S0003-2670(00)88444-5.
- Nolting, R. F., Gerringa, L. J. A., Swagerman, M. J. W., Timmermans, K. R. and De Baar, H. J.

- W. (1998) 'Fe (III) speciation in the high nutrient, low chlorophyll Pacific region of the Southern Ocean', *Marine Chemistry*, 62(3–4), pp. 335–352. doi: 10.1016/S0304-4203(98)00046-2.
- Paerl, H. W. (1984) 'Cyanobacterial carotenoids: their roles in maintaining optimal photosynthetic production among aquatic bloom forming genera', *Oecologia*, 61(2), pp. 143–149. doi: 10.1007/BF00396752.
- Parada, A. E., Needham, D. M. and Fuhrman, J. A. (2016) 'Every base matters: Assessing small subunit rRNA primers for marine microbiomes with mock communities, time series and global field samples', *Environmental Microbiology*, 18(5), pp. 1403–1414. doi: 10.1111/1462-2920.13023.
- Park, Y. H., Fuda, J.-L., Durand, I. and Naveira Garabato, A. C. (2008(a)) 'Internal tides and vertical mixing over the Kerguelen Plateau', *Deep Sea Research Part II: Topical Studies in Oceanography*, 55(5–7), pp. 582–593. doi: 10.1016/j.dsr2.2007.12.027.
- Park, Y. H., Roquet, F., Durand, I. and Fuda, J. L. (2008(b)) 'Large-scale circulation over and around the Northern Kerguelen Plateau', *Deep-Sea Research Part II: Topical Studies in Oceanography*, 55(5–7), pp. 566–581. doi: 10.1016/j.dsr2.2007.12.030.
- Partensky, F., Blanchot, J. and Vaultot, D. (1999(a)) 'Differential distribution and ecology of Prochlorococcus and Synechococcus in oceanic waters : a review', *Bulletin de l'Institut océanographique*, 19(19), pp. 457–475. Available at: <http://cat.inist.fr/?aModele=afficheN&cpsidt=1218663>.
- Partensky, F., Hess, W. R. and Vaultot, D. (1999(b)) 'Prochlorococcus, a marine photosynthetic prokaryote of global significance', *Microbiol.Mol Biol.Rev.*, 63(1), pp. 106–127. doi: doi:1092-2172/99/\$04.00.
- Pinhassi, J., Sala, M. M., Havskum, H., Peters, F., Guadayol, Ò., Malits, A. and Marrasé, C. (2004) 'Changes in bacterioplankton composition under different phytoplankton regimens', *Applied and Environmental Microbiology*, 70(11), pp. 6753–6766. doi: 10.1128/AEM.70.11.6753-6766.2004.
- Polis, G. A. and Strong, D. R. (1996) 'Food Web Complexity and Community Dynamics', *The American Naturalist*, 147(5), pp. 813–846.

- Price, N. M., Ahner, B. A. and Morel, F. M. M. (1994) 'The equatorial Pacific Ocean: Grazer-controlled phytoplankton populations in an iron-limited ecosystem', *Limnology and Oceanography*, 39(3), pp. 520–534. doi: 10.4319/lo.1994.39.3.0520.
- Raes, E. J., Bodrossy, L., van de Kamp, J., Bissett, A. and Waite, A. M. (2017) 'Marine bacterial richness increases towards higher latitudes in the eastern Indian Ocean', *Limnology and Oceanography Letters*. doi: 10.1002/lol2.10058.
- Raes, E. J., Thompson, P. A., McInnes, A. S., Nguyen, H. M., Hardman-mountford, N. and Waite, A. M. (2015) 'Sources of new nitrogen in the Indian Ocean', *Global Biogeochemical Cycles*, 935:8, pp. 1283–1297. doi: 10.1002/2015GB005194. Received.
- Raes, E. J., Waite, A. M., McInnes, A. S., Olsen, H., Nguyen, H. M., Hardman-Mountford, N. and Thompson, P. A. (2014) 'Changes in latitude and dominant diazotrophic community alter N₂ fixation', *Marine Ecology Progress Series*, 516, pp. 85–102. doi: 10.3354/meps11009.
- Raven, J. a (1988) 'The iron and molybdenum use efficiencies of plant growth with different energy, carbon and nitrogen sources', *New Phytologist*, 109(3), pp. 279–288. doi: 10.1111/j.1469-8137.1988.tb04196.x.
- Redfield, A. C. (1958) 'The Biological Control of Chemical Factors in the Environment', *American Scientist*, 46(3), pp. 205–221. Available at: www.jstor.org/stable/27827150.
- Reintjes, G., Arnosti, C., Fuchs, B. M. and Amann, R. (2017) 'An alternative polysaccharide uptake mechanism of marine bacteria', *ISME Journal*. Nature Publishing Group, 11(7), pp. 1640–1650. doi: 10.1038/ismej.2017.26.
- Rognes, T., Flouri, T., Nichols, B., Quince, C. and Mahé, F. (2016) 'VSEARCH: a versatile open source tool for metagenomics', *PeerJ*, 4, p. e2584. doi: 10.7717/peerj.2584.
- Rost, B., Zondervan, I. and Wolf-Gladrow, D. (2008) 'Sensitivity of phytoplankton to future changes in ocean carbonate chemistry: Current knowledge, contradictions and research directions', *Marine Ecology Progress Series*, 373, pp. 227–237. doi: 10.3354/meps07776.
- Sañudo-Wilhelmy, S. A., Kustka, A. B., Gobler, C. J., Hutchins, D. A., Yang, M., Lwiza, K., Burns, J., Capone, D. G., Raven, J. A. and Carpenter, E. J. (2001) 'Phosphorus limitation of nitrogen fixation by *Trichodesmium* in the central Atlantic Ocean', *Nature*, 411(6833), pp. 66–69. doi: 10.1038/35075041.

- Sarmiento, J. L., Gruber, N., Brzezinski, M. A. and Dunne, J. P. (2004) 'High-latitude controls of thermocline nutrients and low latitude biological productivity', *Nature*, 479(7374), pp. 556–556. doi: 10.1038/nature10605.
- Sautya, S., Ingole, B., Jones, D. O. B., Ray, D. and Kameshraj, K. A. (2017) 'First quantitative exploration of benthic megafaunal assemblages on the mid-oceanic ridge system of the Carlsberg Ridge, Indian Ocean', *Journal of the Marine Biological Association of the United Kingdom*, 97(2), pp. 409–417. doi: 10.1017/S0025315416000515.
- Scavotto, R. E., Dziallas, C., Bentzon-Tilia, M., Riemann, L. and Moisander, P. H. (2015) 'Nitrogen-fixing bacteria associated with copepods in coastal waters of the North Atlantic Ocean', *Environmental microbiology*, 17(10), pp. 3754–3765. doi: 10.1111/1462-2920.12777.
- Selph, K. E., Landry, M. R., Allen, C. B., Calbet, A., Christensen, S. and Bidigare, R. R. (2001) 'Microbial community composition and growth dynamics in the Antarctic Polar Front and seasonal ice zone during late spring 1997', *Deep-Sea Research Part II: Topical Studies in Oceanography*, 48(19–20), pp. 4059–4080. doi: 10.1016/S0967-0645(01)00077-7.
- Sheppard, C. R. C., Ateweberhan, M., Bowen, B. W., Carr, P., Chen, C. A., Clubbe, C., Craig, M. T., Ebinghaus, R., Eble, J., Fitzsimmons, N., Gaither, M. R., Gan, C. H., Gollock, M., Guzman, N., Graham, N. A. J., Harris, A., Jones, R., Keshavmurthy, S., Koldewey, H., Lundin, C. G., Mortimer, J. A., Obura, D., Pfeiffer, M., Price, A. R. G., Purkis, S., Raines, P., Readman, J. W., Riegl, B., Rogers, A., Schleyer, M., Seaward, M. R. D., Sheppard, A. L. S., Tamelander, J., Turner, J. R., Visram, S., Vogler, C., Vogt, S., Wolschke, H., Yang, J. M. C., Yang, S. Y. and Yesson, C. (2012) 'Reefs and islands of the Chagos Archipelago, Indian Ocean: Why it is the world's largest no-take marine protected area', *Aquatic Conservation: Marine and Freshwater Ecosystems*, 22(2), pp. 232–261. doi: 10.1002/aqc.1248.
- Sherr, E. B. and Sherr, B. F. (1994) 'Bacterivory and herbivory: Key roles of phagotrophic protists in pelagic food webs', *Microbial Ecology*, 28(2), pp. 223–235. doi: 10.1007/BF00166812.
- Short, S. M., Jenkins, B. D. and Zehr, J. P. (2004) 'Spatial and Temporal Distribution of Two Diazotrophic Bacteria in the Chesapeake Spatial and Temporal Distribution of Two Diazotrophic Bacteria in the Chesapeake Bay', *Applied and environmental microbiology*, 70(4), p. 2186. doi: 10.1128/AEM.70.4.2186.

- Smetacek, V., Assmy, P. and Henjes, J. (2004) 'The role of grazing in structuring Southern Ocean pelagic ecosystems and biogeochemical cycles', *Antarctic Science*, 16(4), pp. 541–558. doi: 10.1017/S0954102004002317.
- Smetacek, V., De Baar, H. J. W., Bathmann, U. V., Lochte, K. and Rutgers Van Der Loeff, M. M. (1997) 'Ecology and biogeochemistry of the Antarctic Circumpolar Current during austral spring: A summary of Southern Ocean JGOFS cruise ANT X/6 of R.V. Polarstern', *Deep-Sea Research Part II: Topical Studies in Oceanography*, 44(1–2), pp. 1–21. doi: 10.1016/S0967-0645(96)00100-2.
- Staal, M., Meysman, F. J. R. and Stal, L. J. (2003) 'Temperature excludes N₂-fixing heterocystous cyanobacteria in the tropical oceans', *Nature*, 425(6957), pp. 504–507. doi: 10.1038/nature01999.
- Sullivan, C. W., Arrigo, K. R., McClain, C. R., Comiso, J. C. and Firestone, J. (1993) 'Distributions of Phytoplankton Blooms in the Southern Ocean', *Science*, 262(5141), pp. 1832–1837. doi: 10.1126/science.262.5141.1832.
- Syrett, P. J. (1981) 'Nitrogen metabolism of microalgae', *Canadian Bulletin of Fisheries and Aquatic Sciences*, 210, pp. 182–210.
- Talmy, D., Martiny, A. C., Hill, C., Hickman, A. E. and Follows, M. J. (2016) 'Microzooplankton regulation of surface ocean POC:PON ratios', *Global Biogeochemical Cycles*, 30(2), pp. 311–332. doi: 10.1002/2015GB005273.
- Tans, P. and Keeling, R. (2018) *Trends in Atmospheric Carbon Dioxide*, Scripps Institution of Oceanography www.esrl.noaa.gov/gmd/ccgg/trends/.
- Teeling, H., Fuchs, B. M., Becher, D., Klockow, C., Gardebrecht, A., Bennke, C. M., Kassabgy, M., Huang, S., Mann, A. J., Waldmann, J., Weber, M., Klindworth, A., Otto, A., Lange, J., Bernhardt, J., Reinsch, C., Hecker, M., Peplies, J., Bockelmann, F. D., Callies, U., Gerdt, G., Wichels, A., Wiltshire, K. H., Glöckner, F. O., Schweder, T. and Amann, R. (2012) 'Substrate-Controlled Succession of Marine Bacterioplankton Populations Induced by a Phytoplankton Bloom', *Science*, 336(May), pp. 608–611. doi: 10.1126/science.1218344.
- Thomas, F., Hehemann, J. H., Rebuffet, E., Czjzek, M. and Michel, G. (2011) 'Environmental and gut Bacteroidetes: The food connection', *Frontiers in Microbiology*, 2(MAY), pp. 1–16.

doi: 10.3389/fmicb.2011.00093.

Thompson, A. W., Foster, R. A., Krupke, A., Carter, B. J., Musat, N., Vaultot, D., Kuypers, M. M. M. and Zehr, J. P. (2012) 'Unicellular Cyanobacterium Symbiotic with a Single-Celled Eukaryotic Alga', *Science*, 337(September), pp. 1546–1550.

Thompson, P. A., Bonham, P., Waite, A. M., Clementson, L. A., Cherukuru, N., Hassler, C. and Doblin, M. A. (2011) 'Deep-Sea Research II Contrasting oceanographic conditions and phytoplankton communities on the east and west coasts of Australia', *Deep-Sea Research Part II*. Elsevier, 58(5), pp. 645–663. doi: 10.1016/j.dsr2.2010.10.003.

Thomson, R. E. and Fine, I. V. (2003) 'Estimating mixed layer depth from oceanic profile data', *Journal of Atmospheric and Oceanic Technology*, 20(2), pp. 319–329. doi: 10.1175/1520-0426(2003)020<0319:EMLDFO>2.0.CO;2.

Torres-Valdes, S., Roussenov, V. M., Sanders, R., Reynolds, S., Pan, X., Mather, R., Landolfi, A., Wolff, G. A., Achterberg, E. P. and Williams, R. G. (2009) 'Distribution of dissolved organic nutrients and their effect on export production over the Atlantic Ocean', *Global Biogeochemical Cycles*, 23, pp. 1–16. doi: 10.1029/2008GB003389.

Tyrrell, T., Merico, A., Waniek, J. J., Wong, C. S., Metzl, N. and Whitney, F. (2005) 'Effect of seafloor depth on phytoplankton blooms in high-nitrate, low-chlorophyll (HNLC) regions', *Journal of Geophysical Research: Biogeosciences*, 110(G2), p. n/a-n/a. doi: 10.1029/2005JG000041.

Uitz, J., Claustre, H., Morel, A. and Hooker, S. B. (2006) 'Vertical distribution of phytoplankton communities in open ocean: An assessment based on surface chlorophyll', *Journal of Geophysical Research: Oceans*, 111(8). doi: 10.1029/2005JC003207.

Vidussi, F., Claustre, H., Manca, B. B., Luchetta, A. and Marty, J.-C. (2001) 'Phytoplankton pigment distribution in relation to upper thermocline circulation in the eastern Mediterranean Sea during winter', *Journal of Geophysical Research*, 106(19), pp. 939–956. doi: 10.1029/1999JC000308.

Voss, M., Bange, H. W., Dippner, J. W., Middelburg, J. J., Montoya, J. P. and Ward, B. (2013) 'The marine nitrogen cycle : recent discoveries , uncertainties and the potential relevance of climate change', *Phil.Trans. R. Soc. B.: Biological Sciences*, 368, p. 20130121.

- Wafar, M., Venkataraman, K., Ingole, B., Khan, S. A. and LokaBharathi, P. (2011) 'State of knowledge of coastal and marine biodiversity of Indian ocean countries', *PLoS ONE*, 6(1). doi: 10.1371/journal.pone.0014613.
- Waite, A. M., Rossi, V., Roughan, M., Tilbrook, B., Thompson, P. A., Feng, M., Wyatt, A. S. J. and Raes, E. J. (2013) 'Formation and maintenance of high-nitrate , low pH layers in the eastern Indian Ocean and the role of nitrogen fixation', *Biogeosciences*, 10, pp. 5691–5702. doi: 10.5194/bg-10-5691-2013.
- Waterbury, J. B., Watson, S. W., Valois, F. W. and Franks, D. G. (1986) 'Biological and ecological characterisation of the marine unicellular cyanobacterium *Synechococcus*', *Canadian Bulletin of Fisheries and Aquatic Sciences*, 214, pp. 71–120.
- Weber, T. S. and Deutsch, C. (2010) 'Ocean nutrient ratios governed by plankton biogeography', *Nature*. Nature Publishing Group, 467(7315), pp. 550–554. doi: 10.1038/nature09403.
- Wilkins, D., Lauro, F. M., Williams, T. J., Demaere, M. Z., Brown, M. V., Hoffman, J. M., Andrews-Pfannkoch, C., Mcquaid, J. B., Riddle, M. J., Rintoul, S. R. and Cavicchioli, R. (2013) 'Biogeographic partitioning of Southern Ocean microorganisms revealed by metagenomics', *Environmental Microbiology*, 15(5), pp. 1318–1333. doi: 10.1111/1462-2920.12035.
- Wood, E. D., Armstrong, F. A. J. and Richards, F. A. (1967) 'Determination of nitrate in sea water by cadmium-copper reduction to nitrite', *Journal of the Marine Biological Association of the United Kingdom*, 47(1), pp. 23–31. doi: 10.1017/S002531540003352X.
- Wyrski, K. (1973) 'Physical Oceanography of the Indian Ocean', in Zeitzschel, B. (ed.) *The Biology of the Indian Ocean*. Ecological Studies 3, pp. 18–36. doi: 10.1007/978-3-642-65468-8.
- Zehr, J. P. and McCreynolds, L. a (1989) 'Use of degenerate oligonucleotides for amplification of the *nifH* gene from the marine cyanobacterium *Trichodermium thiebautii*', *Applied Environmental Microbiology*, 55(10), pp. 2522–2526.
- Zehr, J. P., Waterbury, J. B., Turner, P. J., Montoya, J. P., Omoregie, E., Steward, G. F., Hansen, A. and Karl, D. M. (2001) 'Unicellular cyanobacteria fix N₂ in the subtropical north Pacific Ocean', *Nature*, 412(6847), pp. 635–638. doi: 10.1038/35088063.

Zhang, J., Kobert, K., Flouri, T. and Stamatakis, A. (2014) 'PEAR: A fast and accurate Illumina Paired-End reAd mergeR', *Bioinformatics*, 30(5), pp. 614–620. doi: 10.1093/bioinformatics/btt593.

Appendix

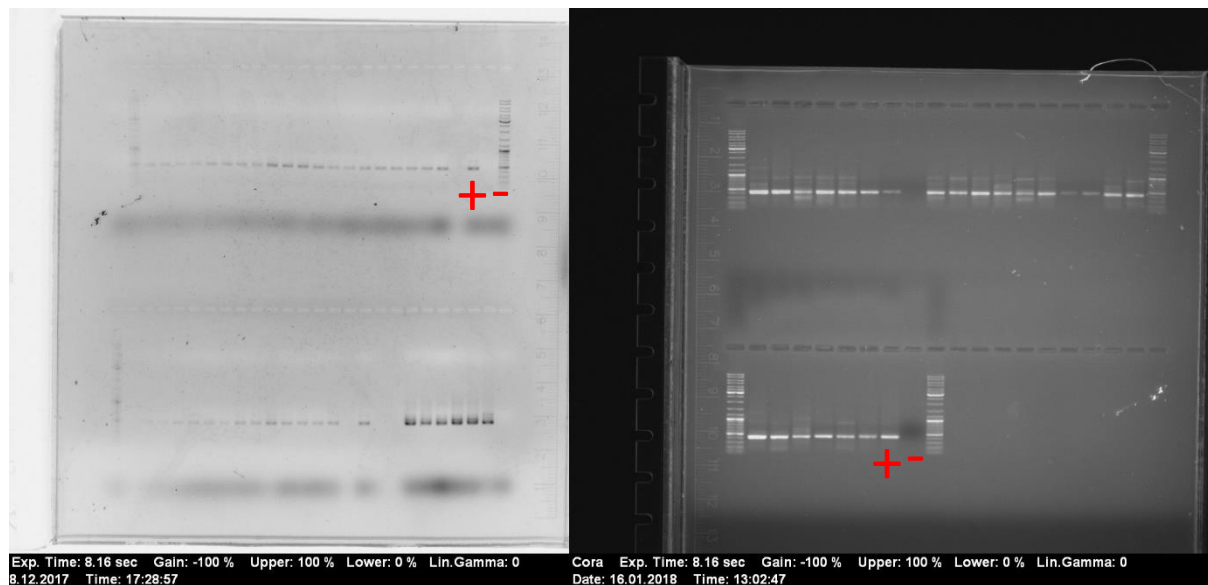


Figure S- 1: gel after (A) 16S and (B) nifH amplicon PCR. A, 16S amplicon PCR. B, nifH amplicon PCR; PCR product was further used for Index PCR. Positive (+) and negative (-) controls worked for both PCR reactions.

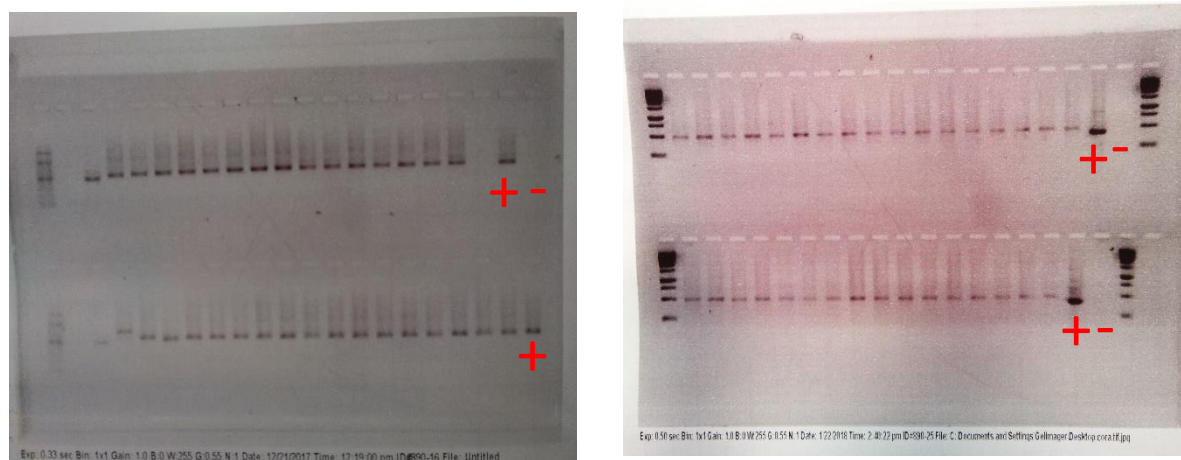


Figure S- 2: gel after (A) 16S and (B) nifH index PCR. negative controls (-) worked for both reactions, old PCR product used as positive control (+).

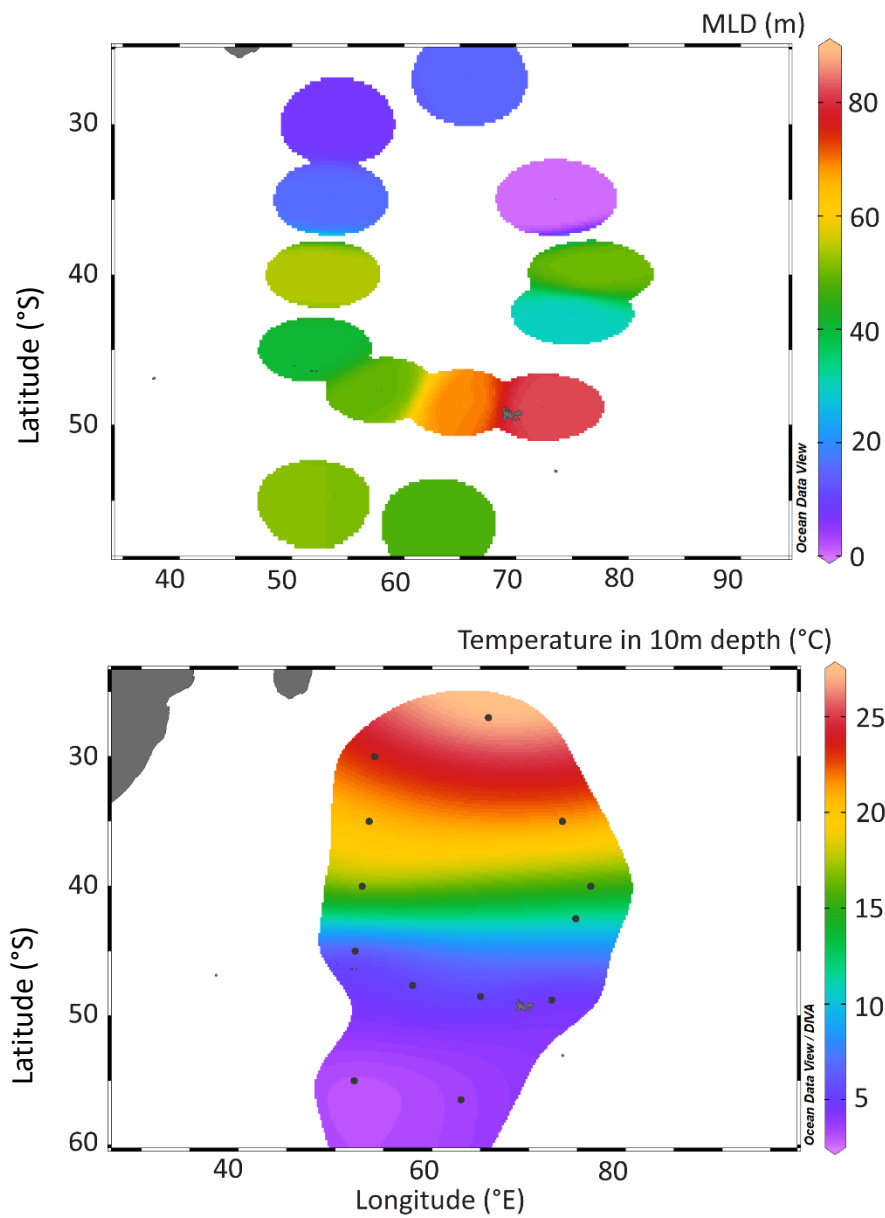


Figure S- 3: Mixed layer depth (MLD) and sea surface temperature (SST) (10m) for all sampling stations. **A,** MLD, showing deepest MLD in the PF around Kerguelen island. **B,** SST, showing clear temperature difference between IO and ACC.

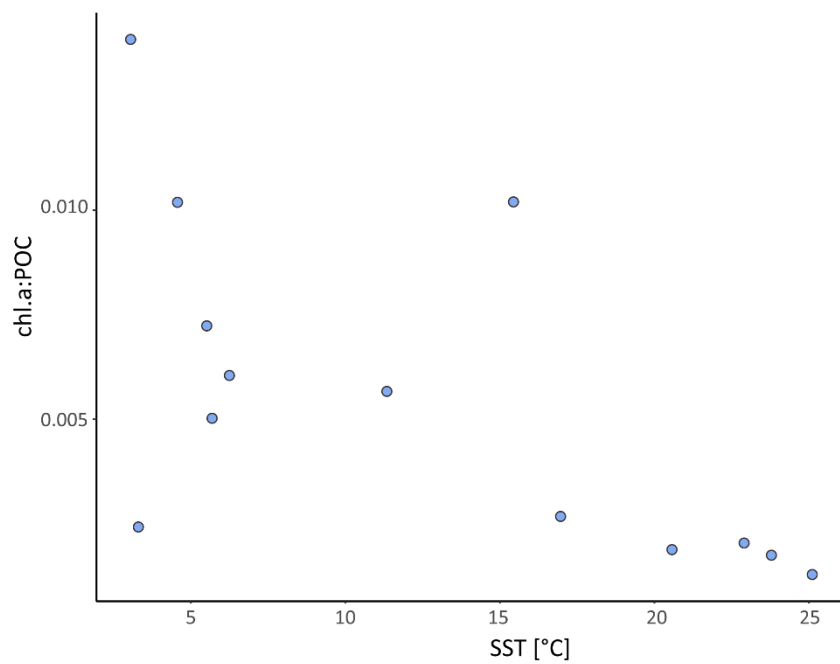


Figure S- 4: relative proportion of chl *a* to total POC against sea surface temperature (SST).

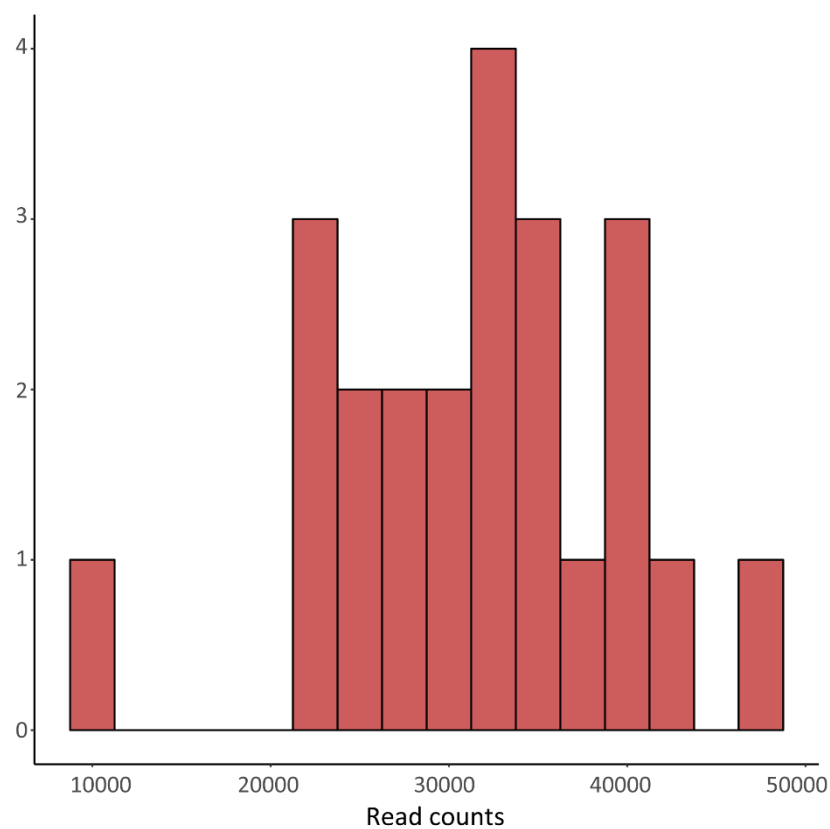


Figure S- 5: Distribution of sample sequencing depth of 16S amplicon sequence data.

Name

Declaration acc. to § 10 Paragraph 11 Common Part of the Master Examination Regulations

I hereby declare that I wrote my Mater Thesis independently and did not use other sources and auxiliary means than the ones indicated.

This Master Thesis is not submitted in another examining procedure.

I further declare that this Master thesis might be made available to the public in this version.

Place/ Date: _____

Signature: _____